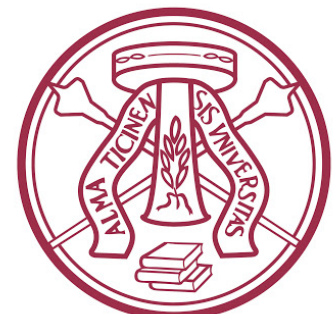


Topical Group on Hadronic Physics

EXPLORING THE PROTON STRUCTURE WITH COMPTON SCATTERING

BARBARA PASQUINI

University of Pavia and INFN Pavia

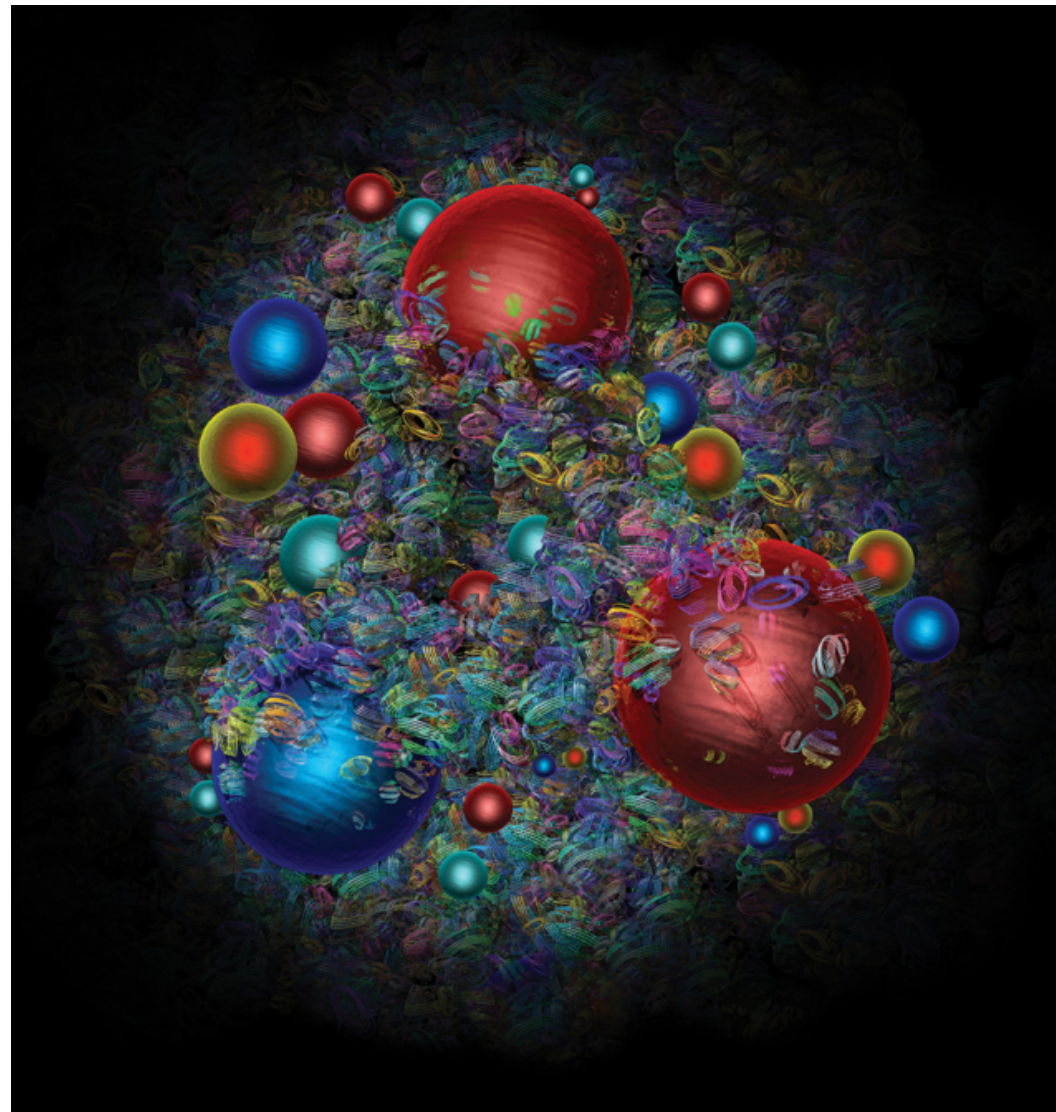


UNIVERSITÀ
DI PAVIA



``What proton is depends on how you look at it, or rather on how hard you hit it''

A. Cooper-Sarkar, CERN Courier, June, 2019



Resolution scale

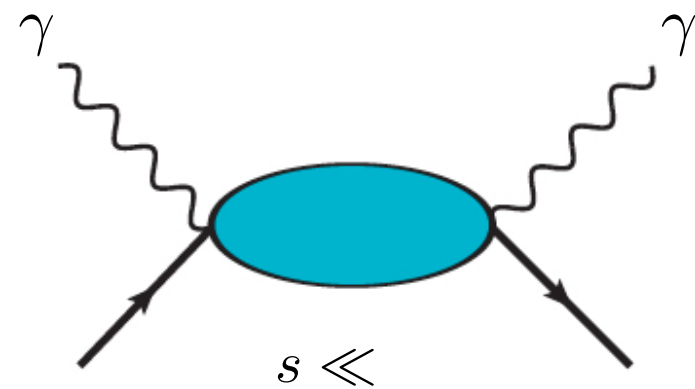
hadronic d.o.f.

nucleon resonances

partonic d.o.f. 

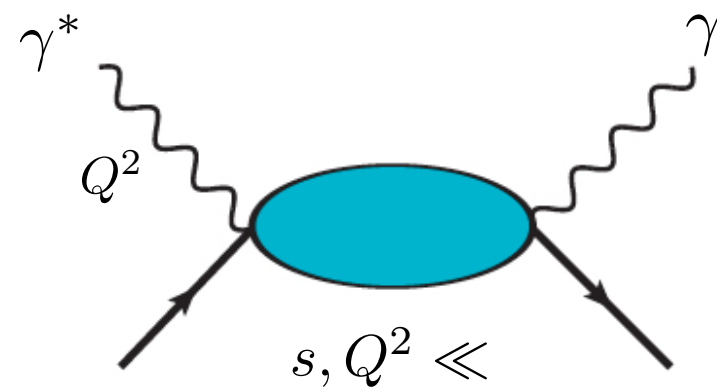
How can we explain the evolving picture of hadrons
from low to high resolution scale?

RCS polarizabilities



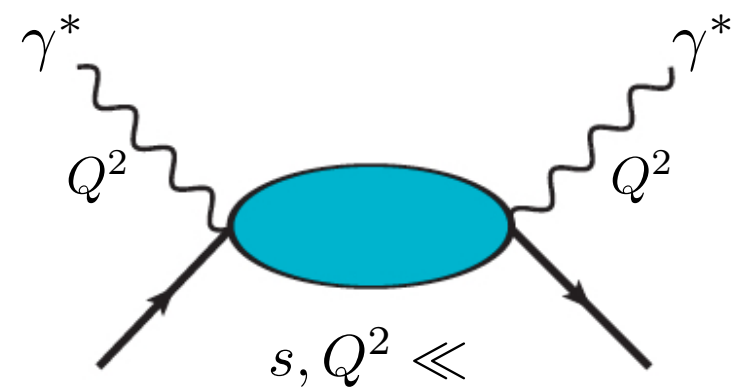
global response

VCS generalized pol.



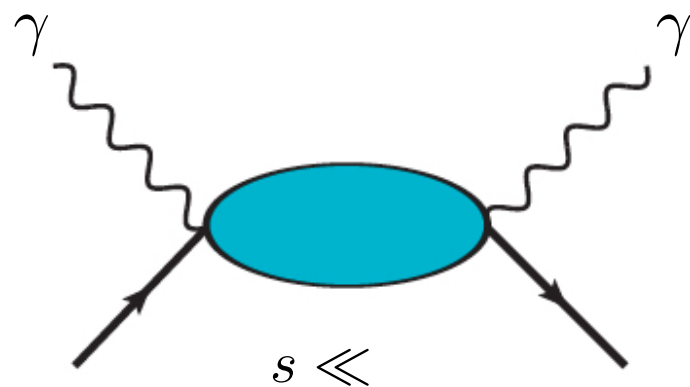
local response
on a distance scale depending on Q^2

VVCS generalized pol.

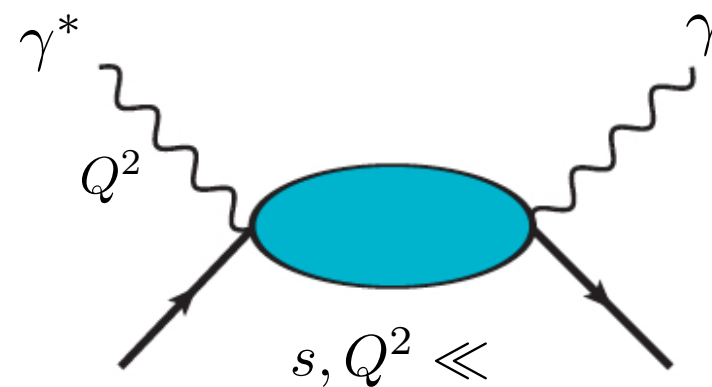


inclusive inelastic
structure functions

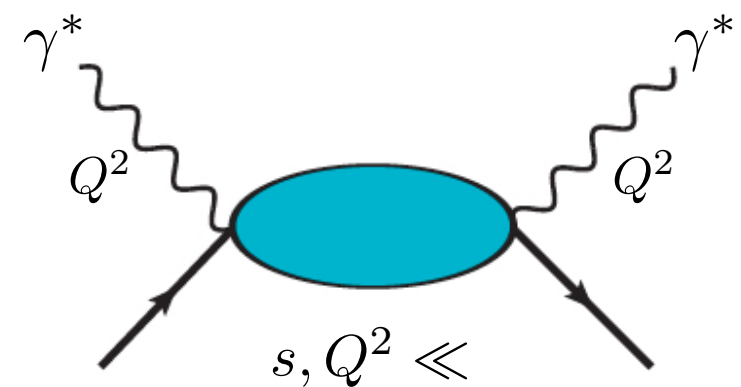
RCS polarizabilities



VCS generalized pol.

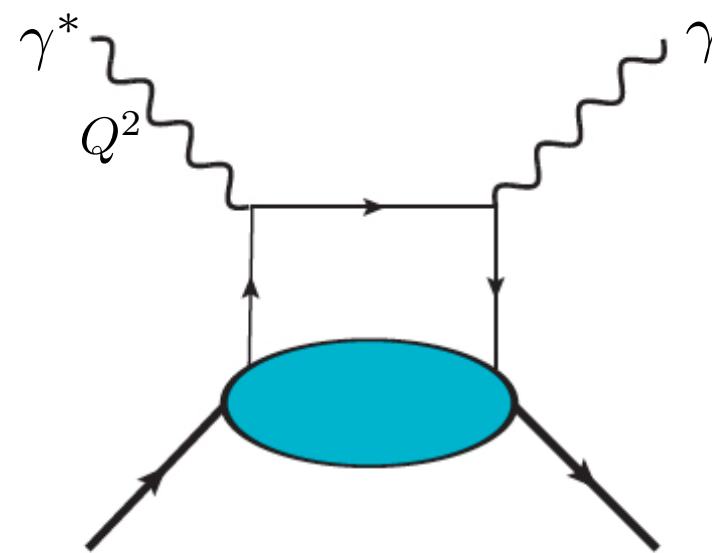


VVCS generalized pol.

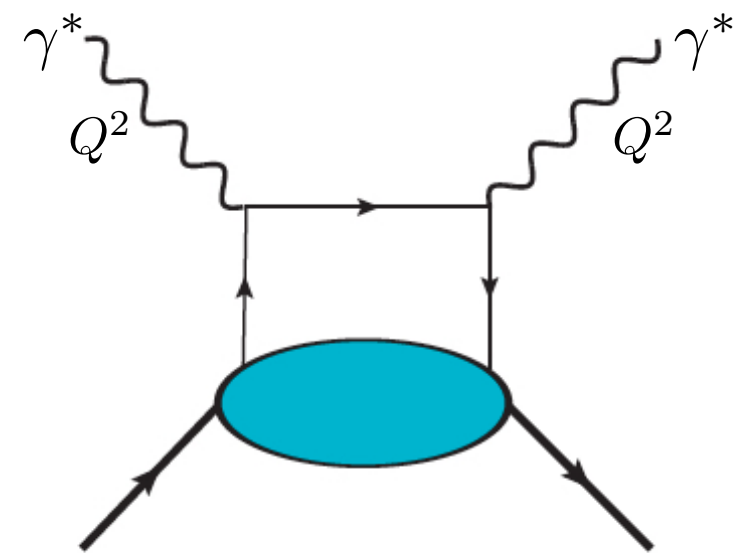


$s, Q^2 \gg$

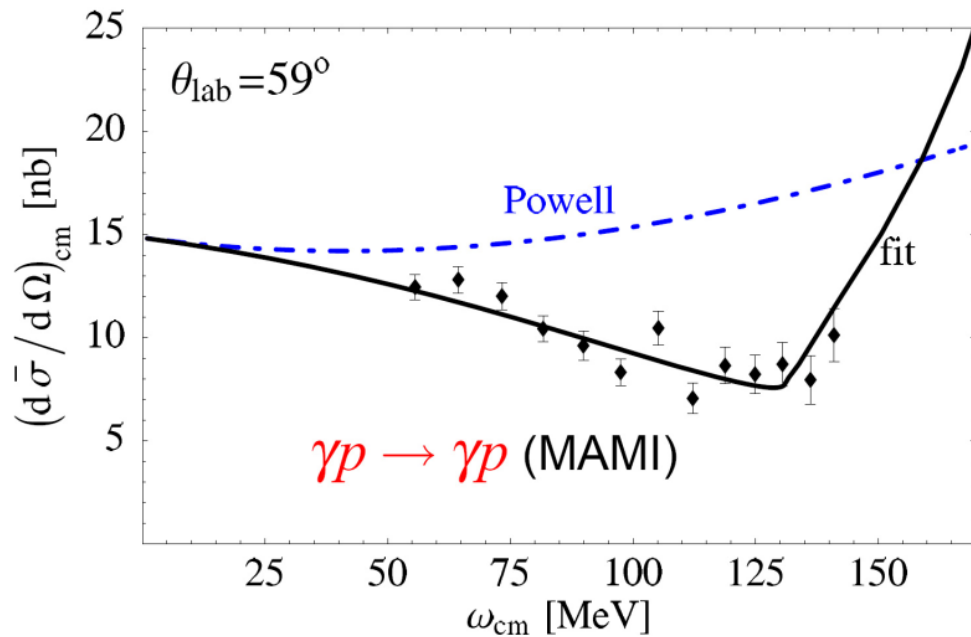
DVCS
generalized parton distributions



DIS
parton distributions

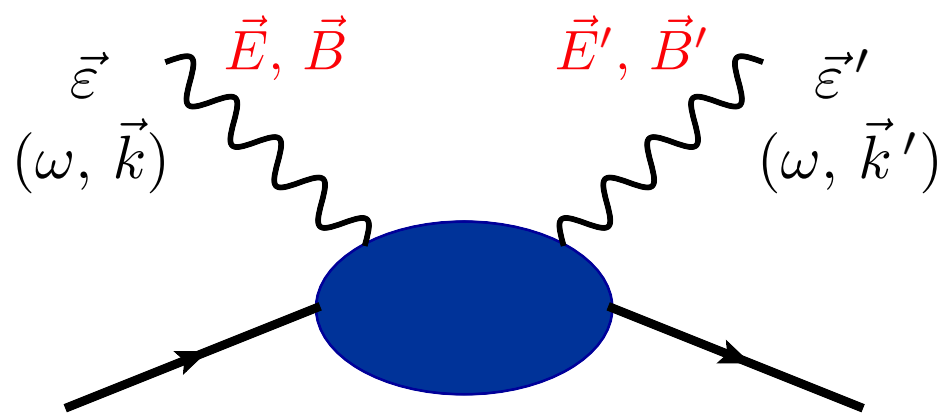


Real Compton Scattering at low energies



Powell cross section: photon scattering off a pointlike nucleon with anomalous magnetic moment

Static polarizabilities: response of the internal nucleon degrees of freedom to a static electric and magnetic field



$$\begin{aligned}
 H_{\text{eff}}^{\text{pol.}} = & -2\pi \left\{ \omega^2 \left[\alpha_{E1} \vec{E}^2 + \beta_{M1} \vec{B}^2 \right] \right. \\
 & + \omega^3 \left[\gamma_{E1E1} \vec{\sigma} \cdot (\vec{E} \times \dot{\vec{E}}) + \gamma_{M1M1} \vec{\sigma} \cdot (\vec{B} \times \dot{\vec{B}}) \right. \\
 & \left. \left. - 2\gamma_{M1E2} \sigma_i B_j E_{ij} + 2\gamma_{E1M2} \sigma_i E_j B_{ij} \right] + \mathcal{O}(\omega^3) \right\}
 \end{aligned}$$

spin-independent dipole

spin-dependent dipole

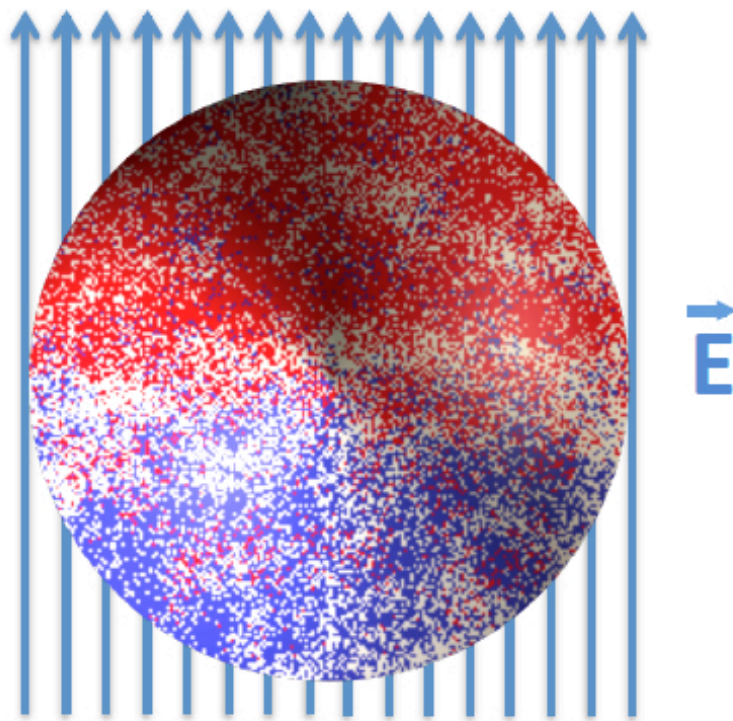
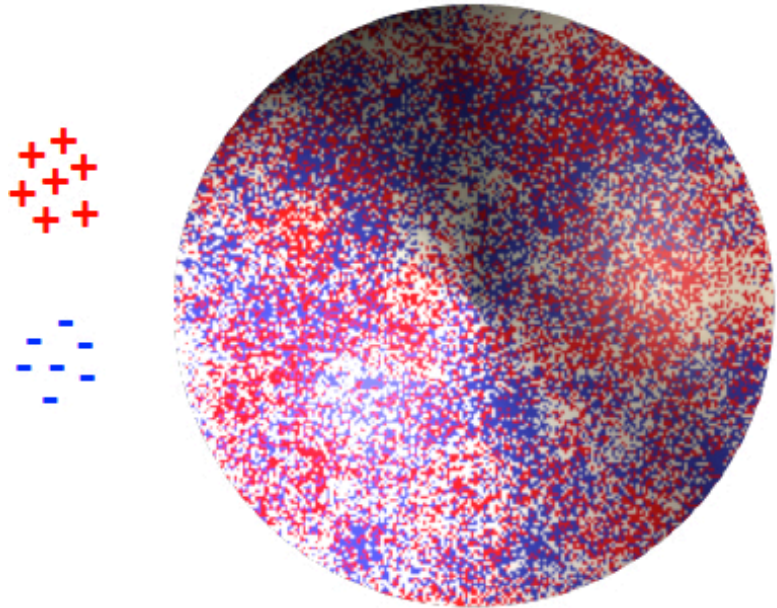
spin-dependent dipole-quadrupole

RCS Polarizabilities

Measure of the strength of induced polarizations: 2 scalar polarizabilities + 4 spin polarizabilities

RCS Polarizabilities

Measure of the strength of induced polarizations: 2 scalar polarizabilities + 4 spin polarizabilities



$$\vec{D}_E \sim \alpha_{E1} \vec{E}$$

Unlike atoms,
it is not proportional to volume

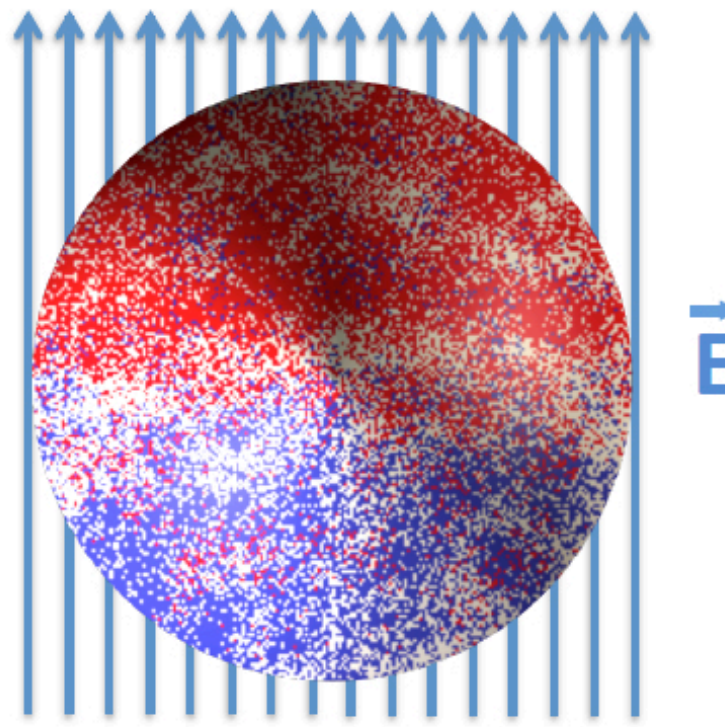
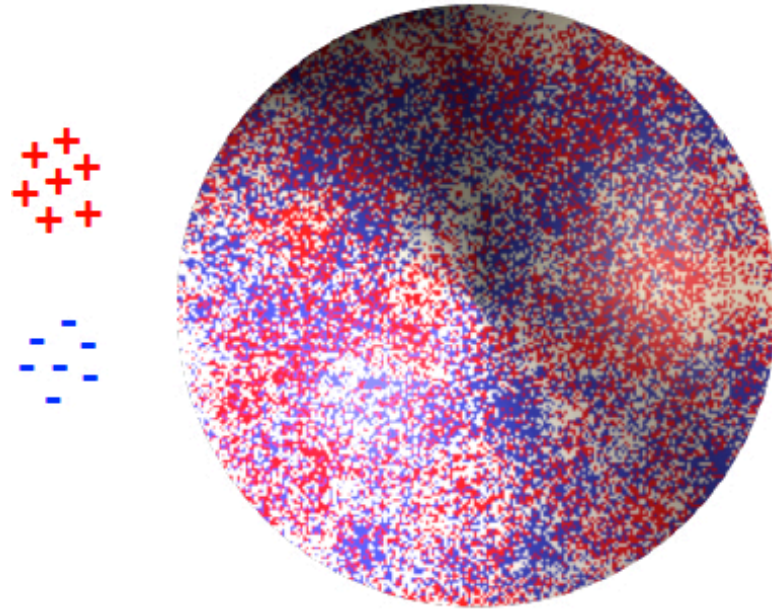
$$V \sim \langle r_p \rangle^3 \approx 0.6 \text{ fm}^3$$

$$\alpha_{E1} \approx 10^{-4} V_p$$

much ``stiffer'' than hydrogen!

RCS Polarizabilities

Measure of the strength of induced polarizations: 2 scalar polarizabilities + 4 spin polarizabilities



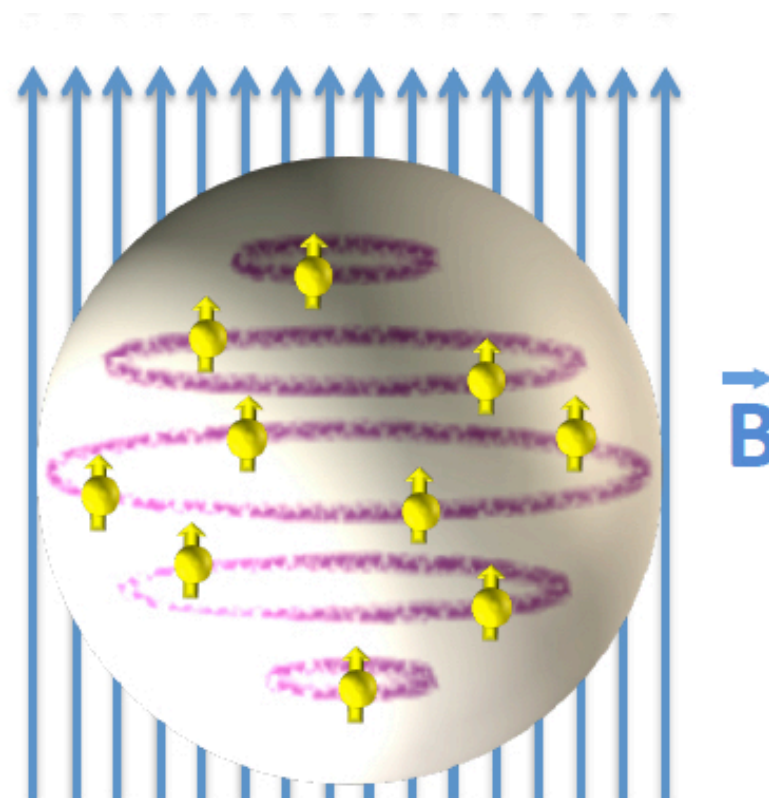
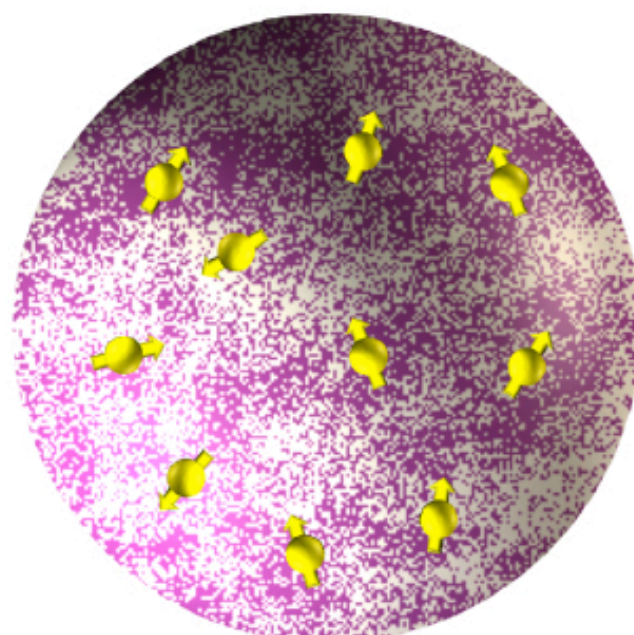
$$\vec{D}_E \sim \alpha_{E1} \vec{E}$$

Unlike atoms,
it is not proportional to volume

$$V \sim \langle r_p \rangle^3 \approx 0.6 \text{ fm}^3$$

$$\alpha_{E1} \approx 10^{-4} V_p$$

much ``stiffer'' than hydrogen!



$$\vec{D}_M \sim \beta_{M1} \vec{B}$$

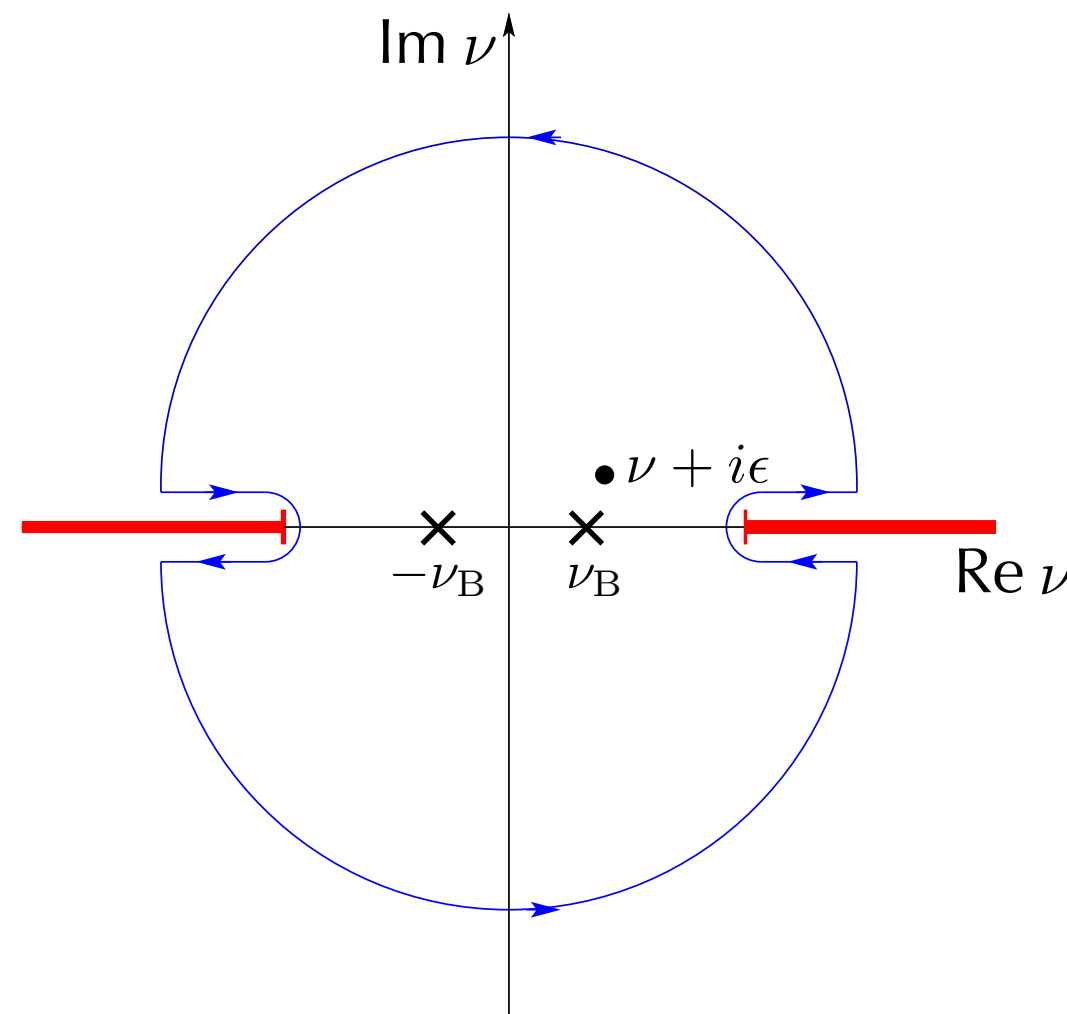
$\beta_{M1}^{\text{para}} > 0$ proton spin aligns
with external field

$\beta_{M1}^{\text{dia}} < 0$ induced current
of pion cloud generates field
opposite to the external one

Dispersion Relations at fixed t

$A_i(\nu, t)$: 6 analytical functions in the complex ν plane, with cuts and poles on the real axis

$$\nu = E_\gamma + \frac{t}{4M}$$



- Cauchy integral formula

$$A_i(\nu, t, Q^2) = \oint_C d\nu' \frac{A_i(\nu', t, Q^2)}{\nu' - \nu}$$

- Crossing symmetry and analyticity

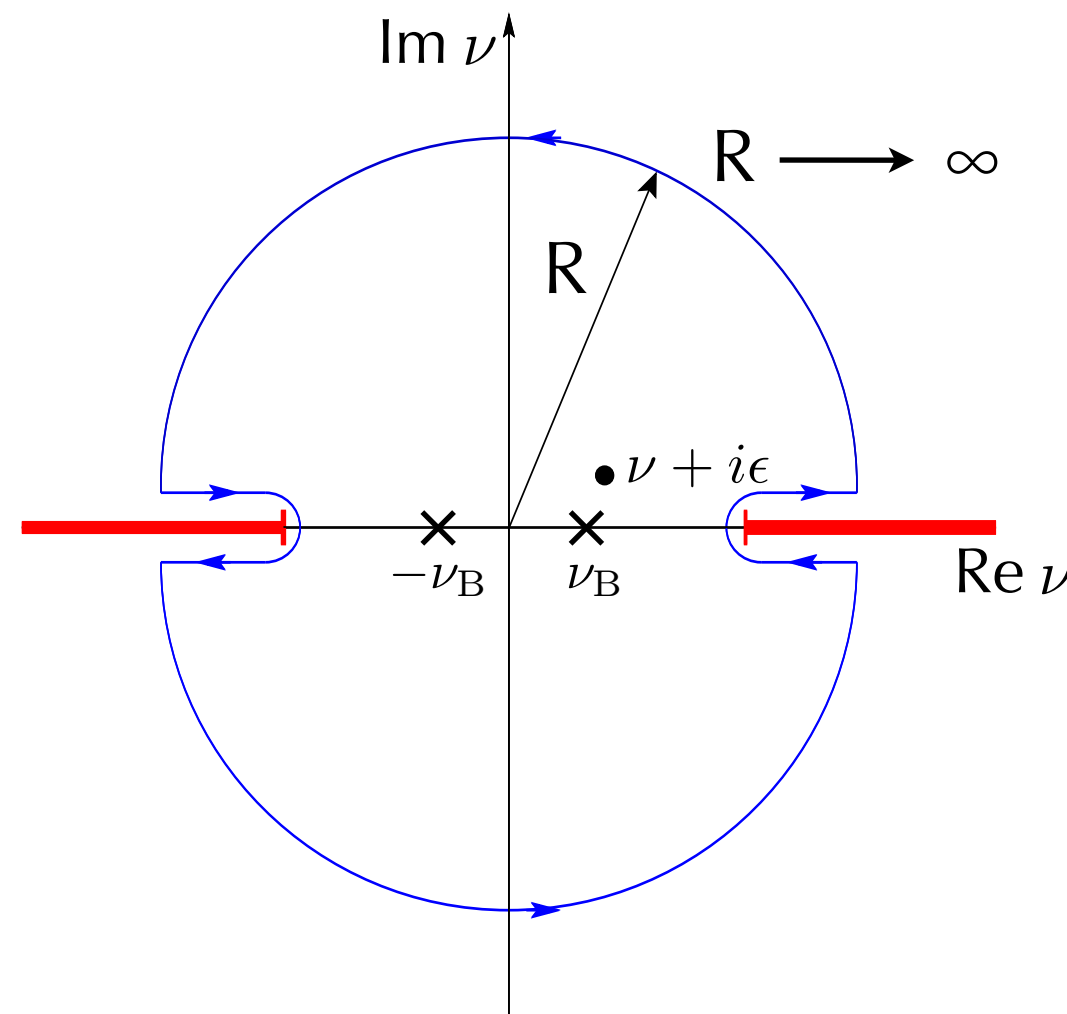
$$A_i(\nu, t, Q^2) = A_i(-\nu, t, Q^2)$$

$$A_i(\nu^*, t, Q^2) = A_i^*(\nu, t, Q^2)$$

Dispersion Relations at fixed t

$A_i(\nu, t)$: 6 analytical functions in the complex ν plane, with cuts and poles on the real axis

$$\nu = E_\gamma + \frac{t}{4M}$$



- Cauchy integral formula

$$A_i(\nu, t, Q^2) = \oint_C d\nu' \frac{A_i(\nu', t, Q^2)}{\nu' - \nu}$$

- Crossing symmetry and analyticity

$$A_i(\nu, t, Q^2) = A_i(-\nu, t, Q^2)$$

$$A_i(\nu^*, t, Q^2) = A_i^*(\nu, t, Q^2)$$

UNsubtracted Dispersion Relations

$$\text{Re } A_i^{\text{NB}}(\nu, t) = \frac{2}{\pi} P \int_{\nu_{thr}}^{\infty} \text{Im}_s A_i(\nu', t) \frac{\nu' d\nu'}{\nu'^2 - \nu^2}$$

non-convergent integrals



SUBtracted Dispersion Relations

$$\text{Re } A_i^{\text{NB}}(\nu, t) = A_i^{\text{NB}}(0, t) + \frac{2}{\pi} \nu^2 P \int_{\nu_{thr}}^{\infty} \text{Im}_s A_i(\nu', t) \frac{d\nu'}{\nu'(\nu'^2 - \nu^2)}$$



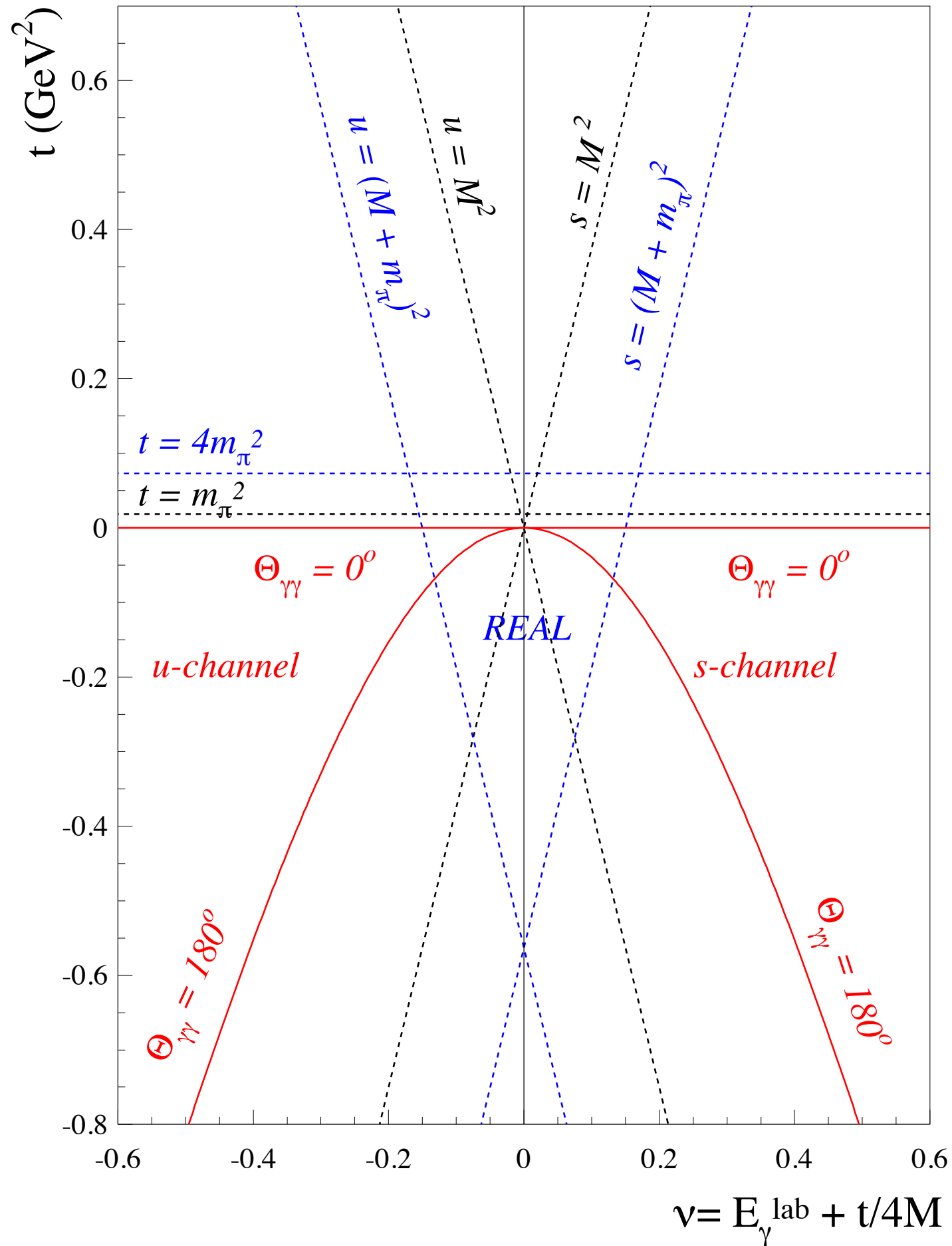
subtraction at $\nu = 0$

$$A_i^{\text{NB}}(0, t) = A_i^{\text{NB}}(0, 0) + \text{t-channel SUBtracted dispersion integrals}$$

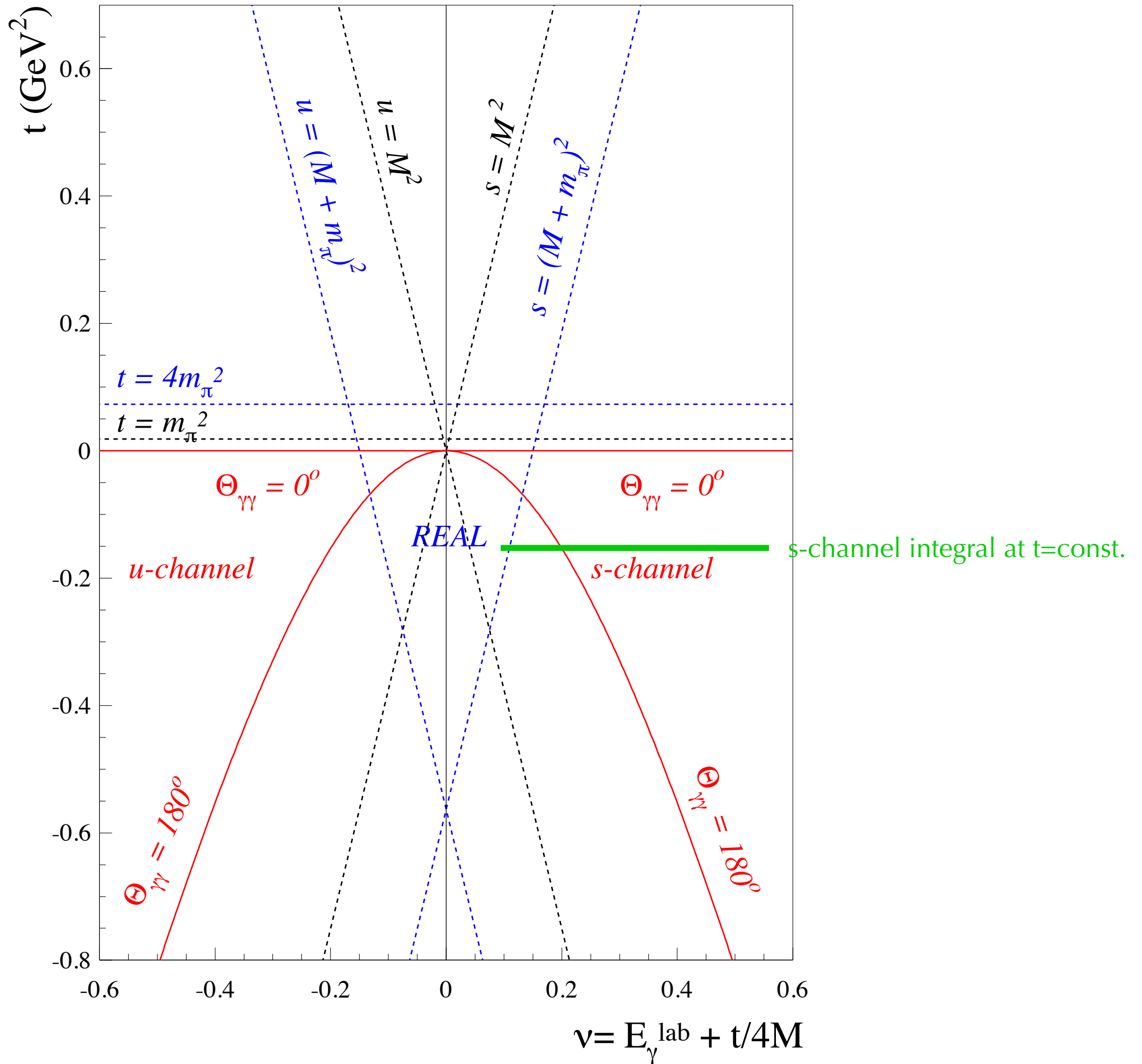


subtraction at $t = 0$

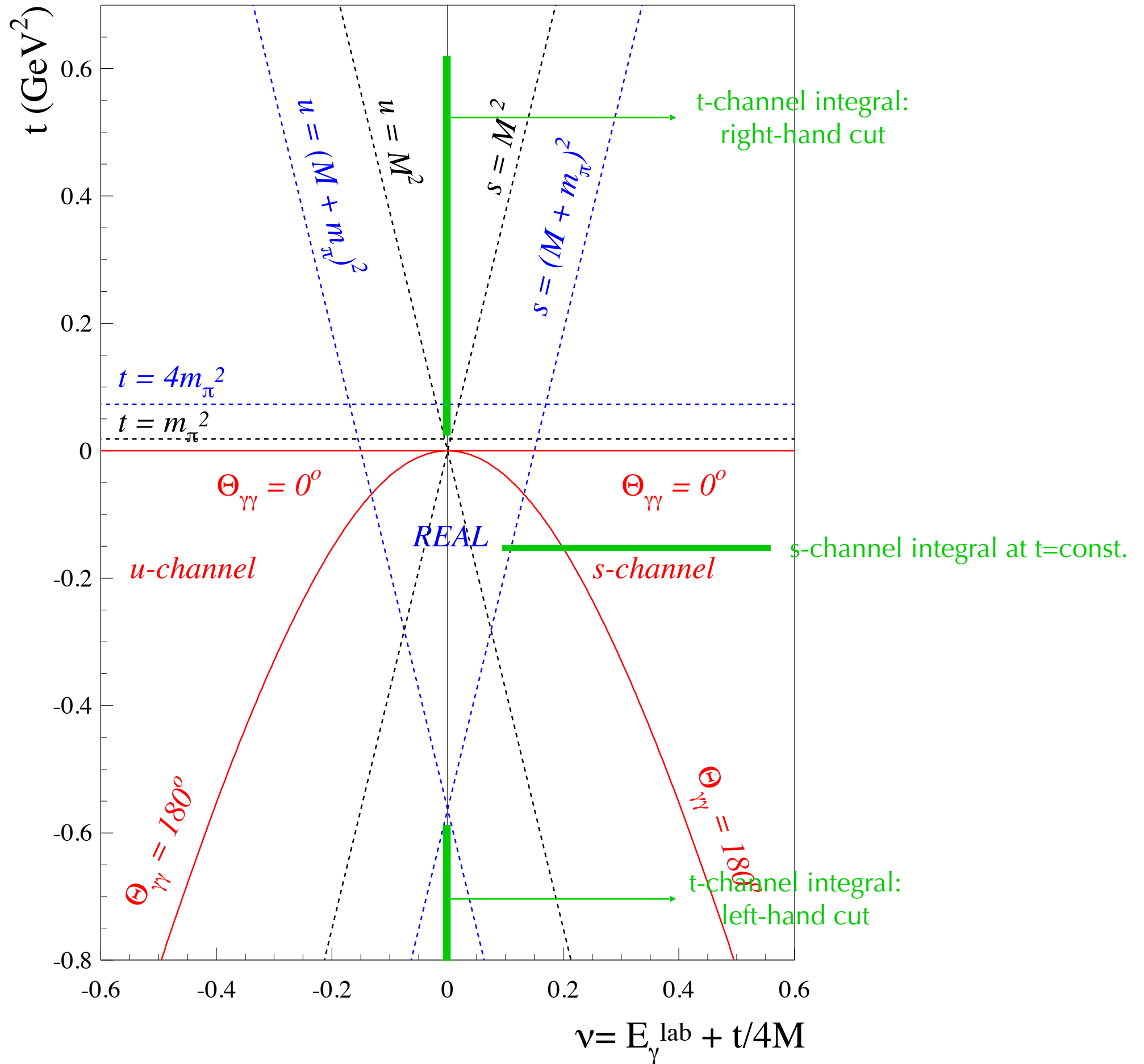
Mandelstam plane for RCS



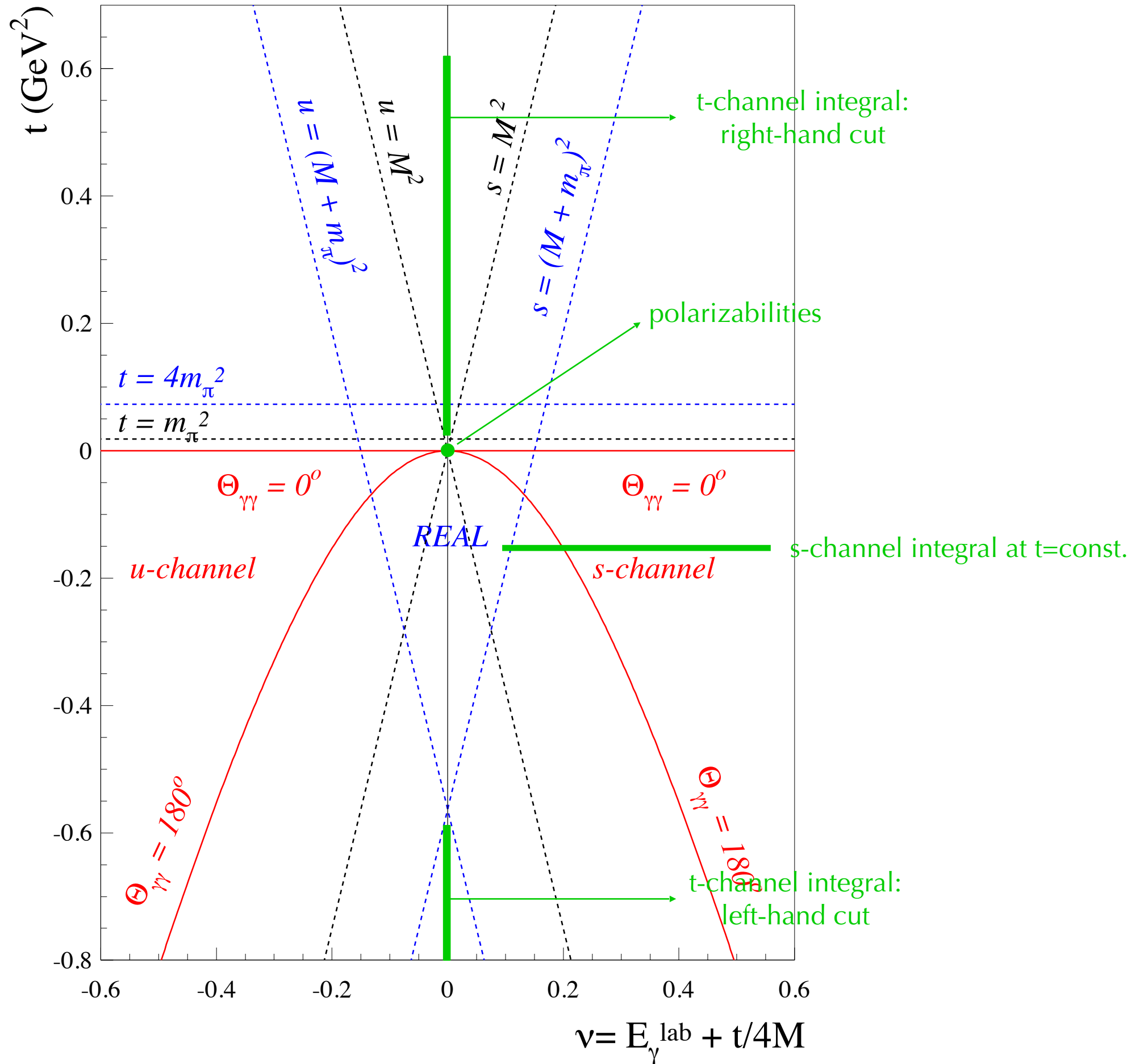
Mandelstam plane for RCS



Mandelstam plane for RCS



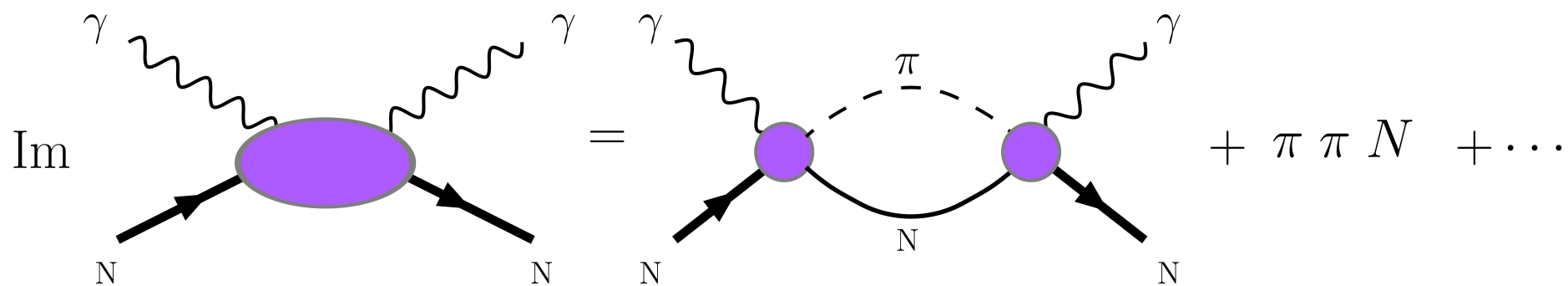
Mandelstam plane for RCS



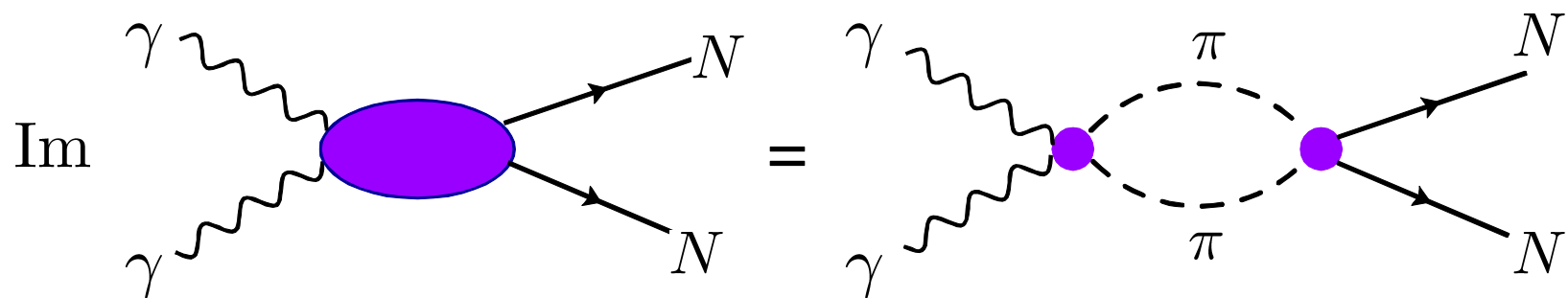
Subtracted Dispersion Relations

$$A_i(\nu, t) = A_i^s(\nu, 0) + A_i^t(0, t) + A_i(0, 0)$$

- $A_i^s(\nu, 0)$ → subtracted dispersion relations in the s-channel



- $A_i^t(0, t)$ → subtracted dispersion relations in the t-channel $\gamma\gamma \rightarrow NN$



- $A_i(0, 0)$ → polarizabilities: free parameters fitted to data

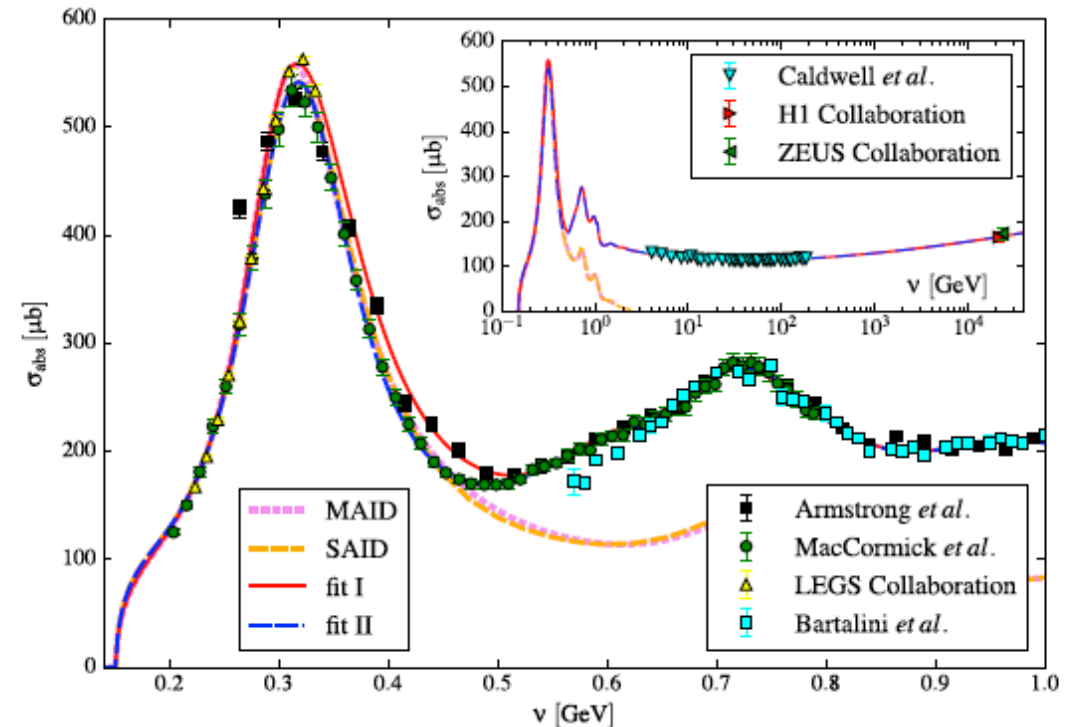
Constraints on the RCS polarizabilities

Baldin sum rule

$$\alpha_{E1} + \beta_{M1} = \frac{1}{2\pi^2} \int_{\nu_{thr}}^{\infty} \frac{\sigma_{1/2} + \sigma_{3/2}}{\nu^2} d\nu$$

$$\alpha_{E1} + \beta_{M1} = (13.8 \pm 0.4) \times 10^{-4} \text{ fm}^3$$

A1 Coll. (MAMI), EPJA10 (2011)



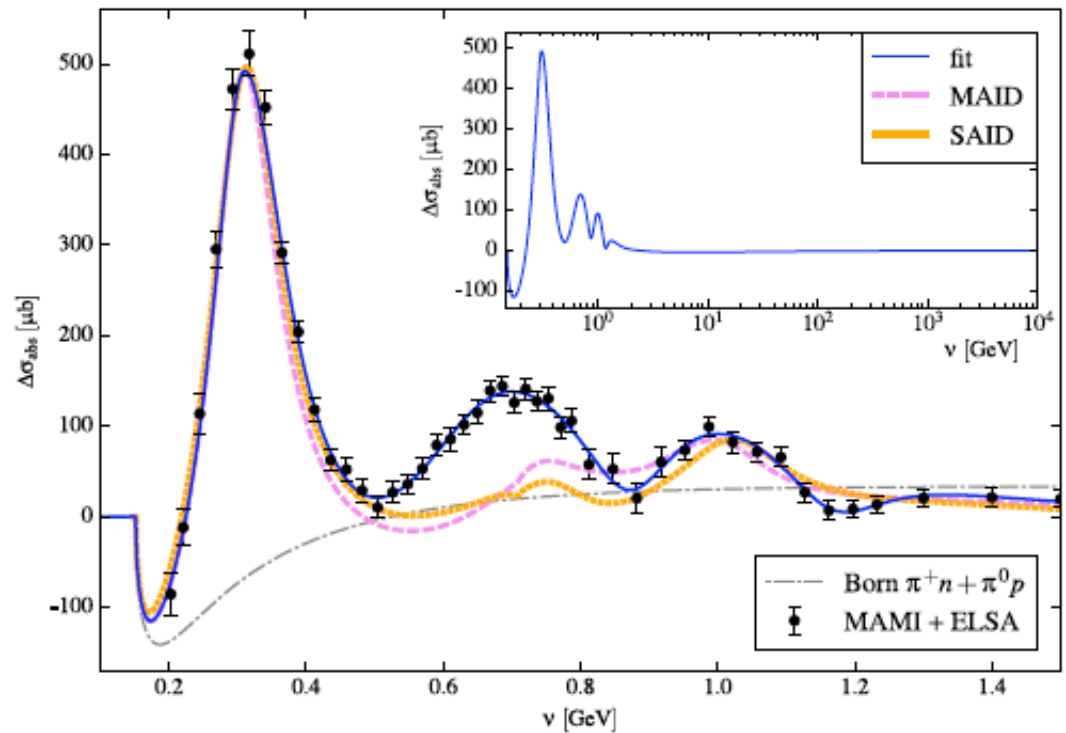
GGT sum rule

$$\gamma_0 = \frac{1}{4\pi^2} \int_{\nu_{thr}}^{\infty} \frac{\sigma_{1/2} - \sigma_{3/2}}{\nu^3} d\nu$$

$$\gamma_0 = -\gamma_{E1E1} - \gamma_{M1M1} - \gamma_{E1M2} - \gamma_{M1E2}$$

$$\gamma_0 = (-1.01 \pm 0.08) \times 10^{-4} \text{ fm}^4$$

BP, Pedroni, Drechsel, PLB687 (2010)



RCS data above threshold

$$\gamma_\pi = \gamma_{E1E1} + \gamma_{M1M1} - \gamma_{E1M2} + \gamma_{M1E2}$$

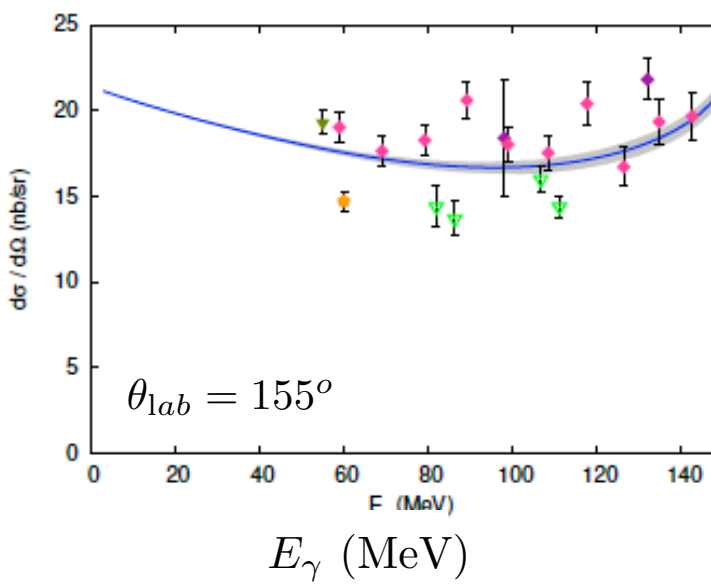
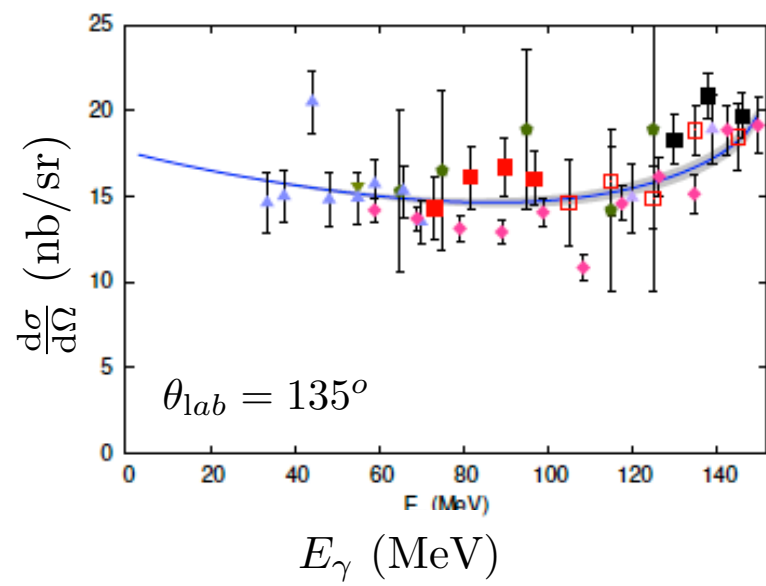
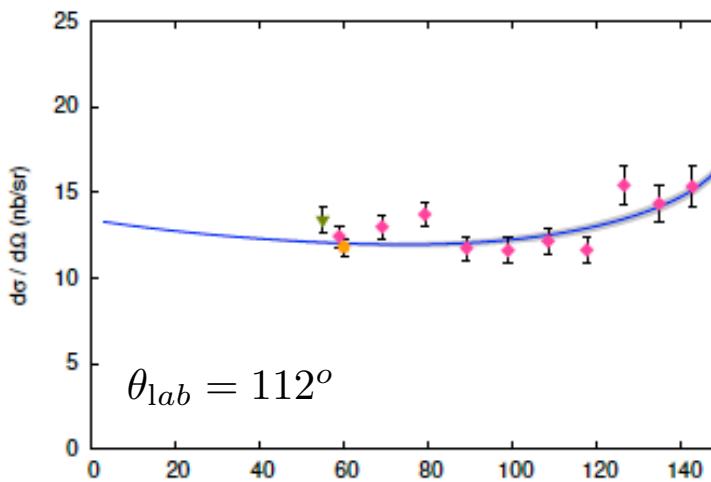
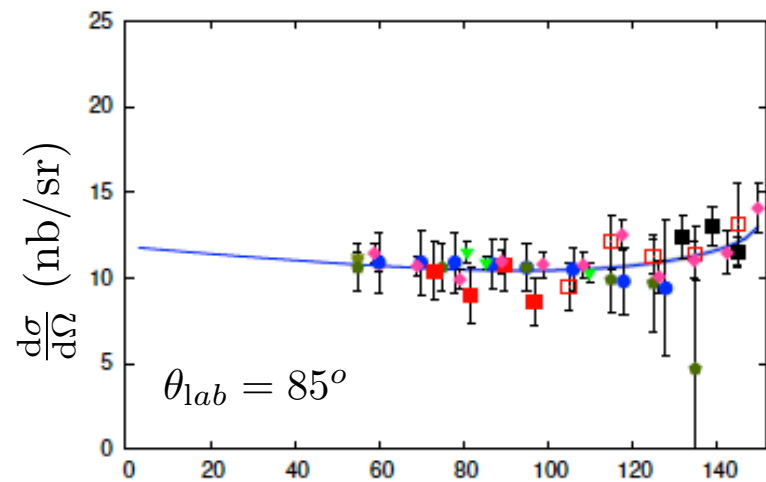
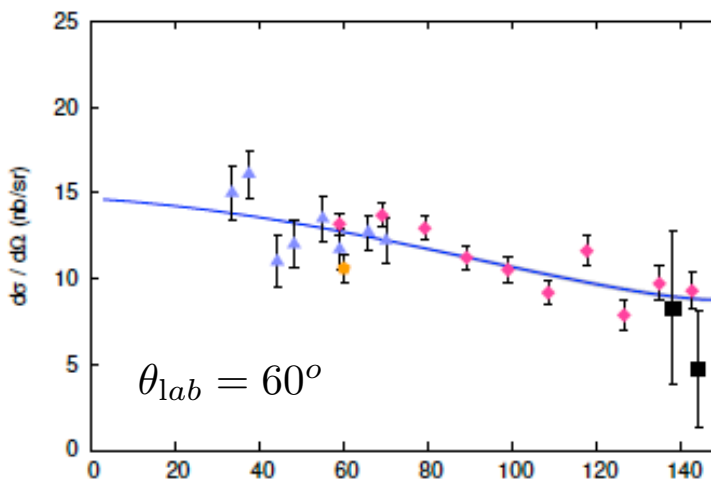
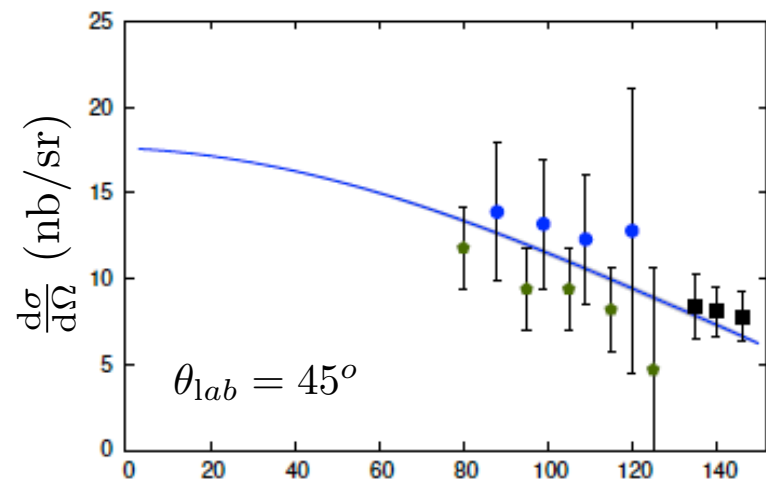
$$\gamma_\pi = (-38.7 \pm 1.8) \times 10^{-4} \text{ fm}^4$$

Schumacher, Prog. Part. Nucl. Phys. 55 (2005)

RCS fit below pion-production threshold

α_{E1} and β_{M1}
free parameters

spin polarizabilities
fixed
from sum rules
and DRs



Status of RCS scalar polarizabilities

Extractions from
different theoretical models:

- BChPT
Lensky et al. [2014]
- HBChPT
McGovern et al. [2013]
- sDRs
Pasquini et al. [2019]

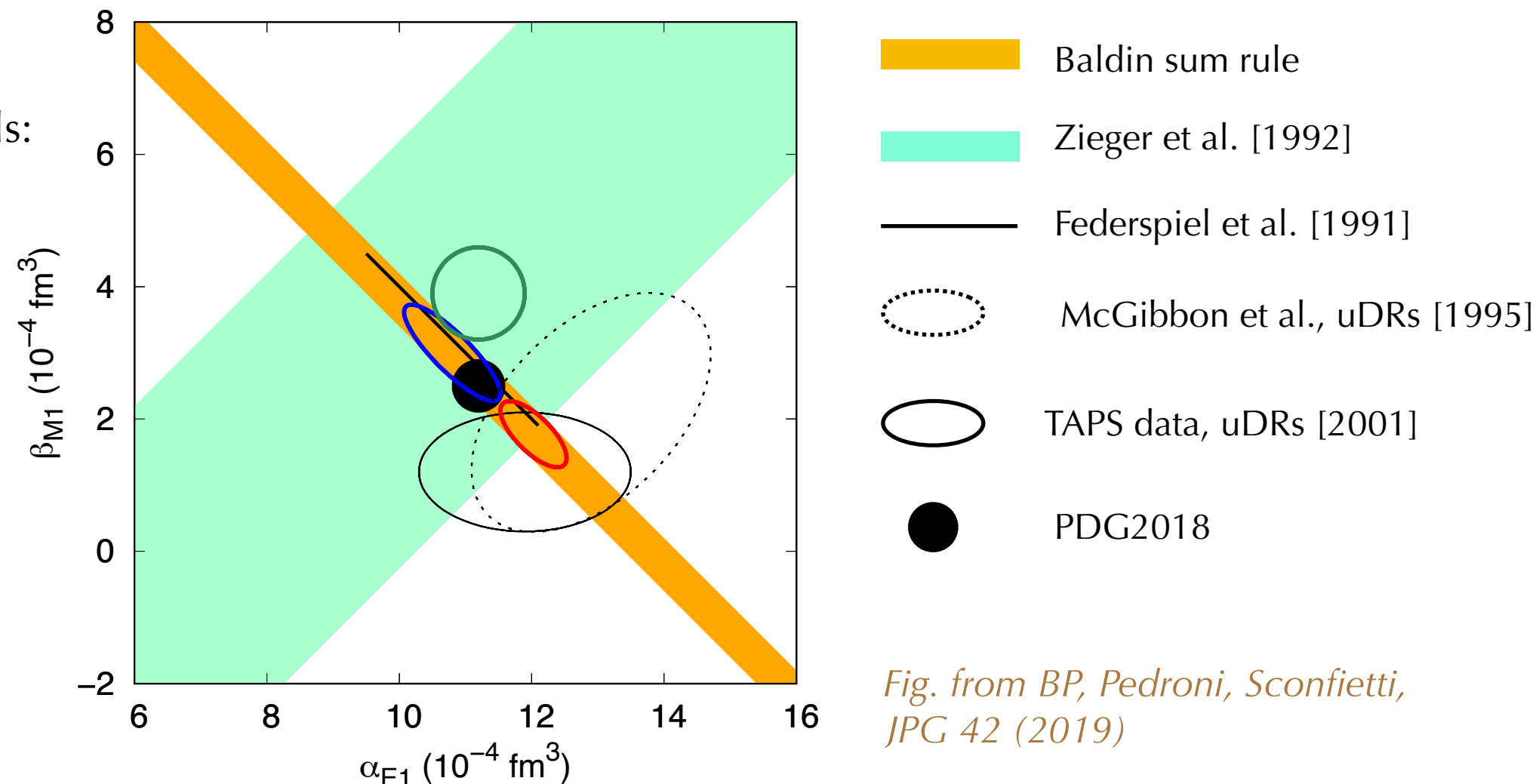


*Fig. from BP, Pedroni, Sconfietti,
JPG 42 (2019)*

PDG2018: $\alpha_{E1} = 11.2 \pm 0.4$ $\beta_{M1} = 2.5 \pm 0.4$

Baldin sum rule: $\alpha_{E1} + \beta_{M1} = 13.8 \pm 0.4$

New extraction with Subtracted Dispersion Relations:

$$\alpha_{E1} = 12.03^{+0.48}_{-0.54}$$

$$\beta_{M1} = 1.77^{+0.52}_{-0.54}$$

BP, Pedroni, Sconfietti, JPG 42 (2019) and to appear in PDG 2021

Status of RCS scalar polarizabilities

Extractions from different theoretical models:

- BChPT
Lensky et al. [2014]
- HBChPT
McGovern et al. [2013]
- sDRs
Pasquini et al. [2019]

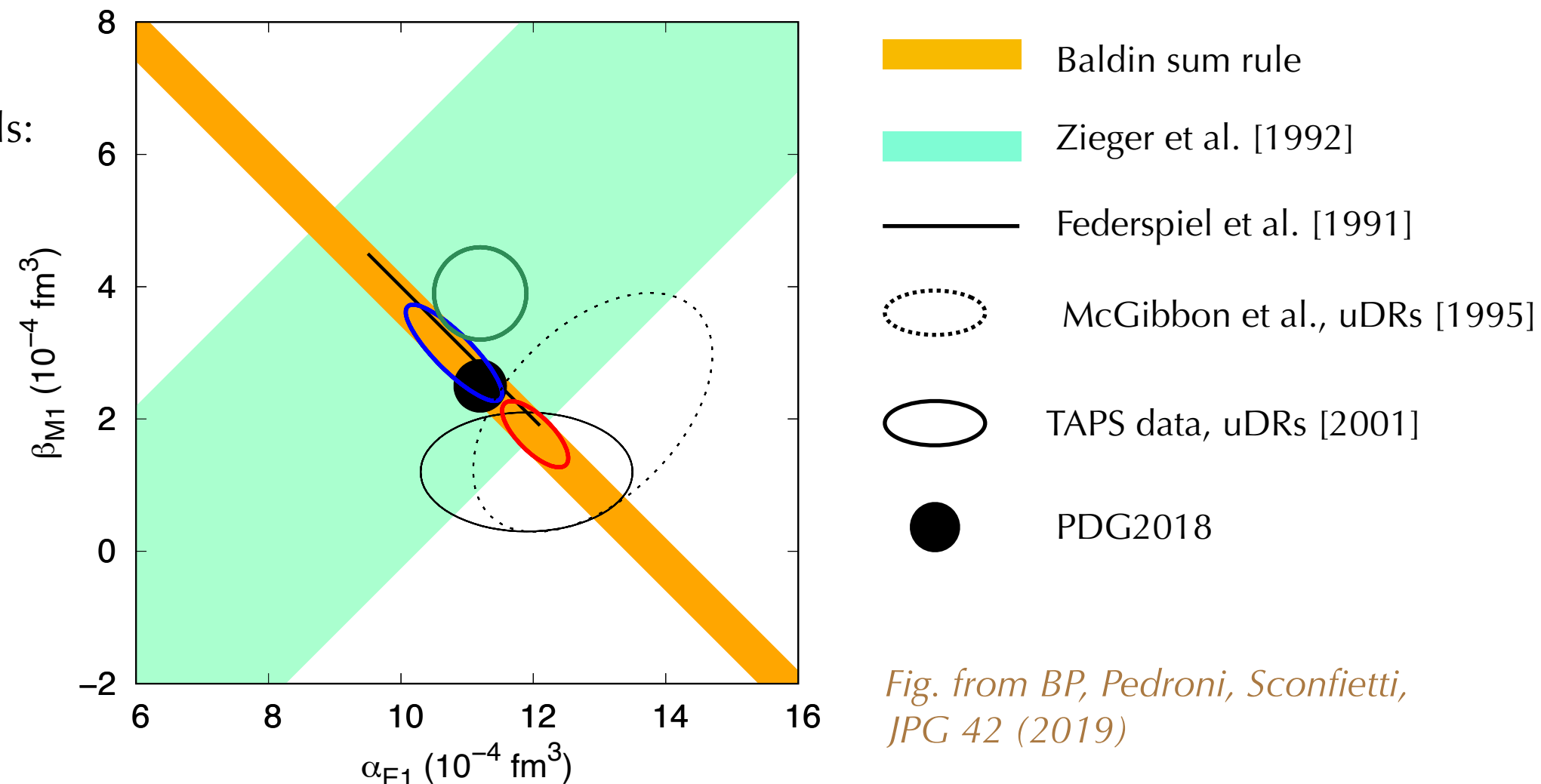


*Fig. from BP, Pedroni, Sconfietti,
JPG 42 (2019)*

PDG2018: $\alpha_{E1} = 11.2 \pm 0.4$ $\beta_{M1} = 2.5 \pm 0.4$

Baldin sum rule: $\alpha_{E1} + \beta_{M1} = 13.8 \pm 0.4$

New extraction with Subtracted Dispersion Relations:

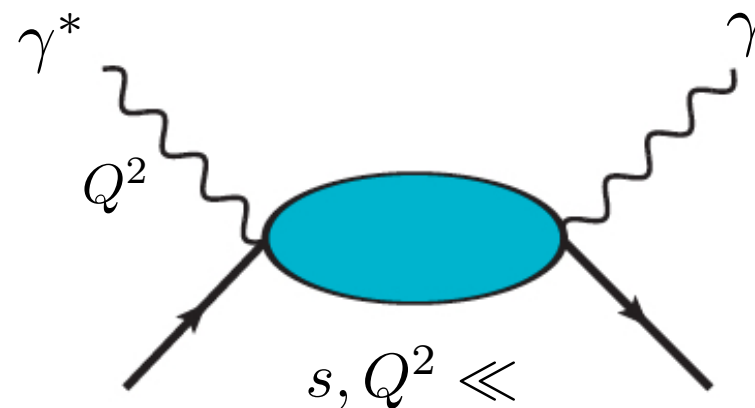
$$\alpha_{E1} = 12.03^{+0.48}_{-0.54}$$

$$\beta_{M1} = 1.77^{+0.52}_{-0.54}$$

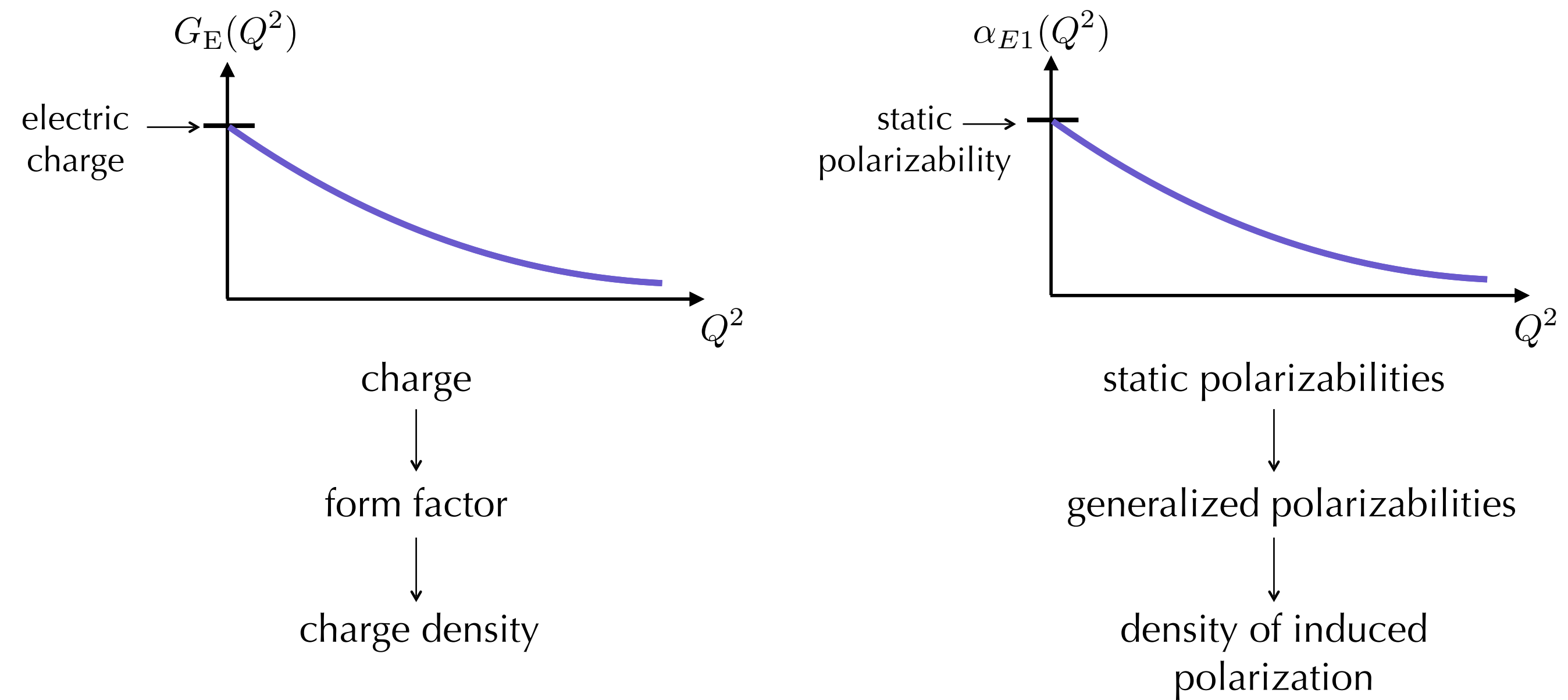
BP, Pedroni, Sconfietti, JPG 42 (2019) and to appear in PDG 2021

DRs used also for the first extraction of spin pol.: A2 Coll. (MAMI), PRC102 (2020); PRL114 (2015)

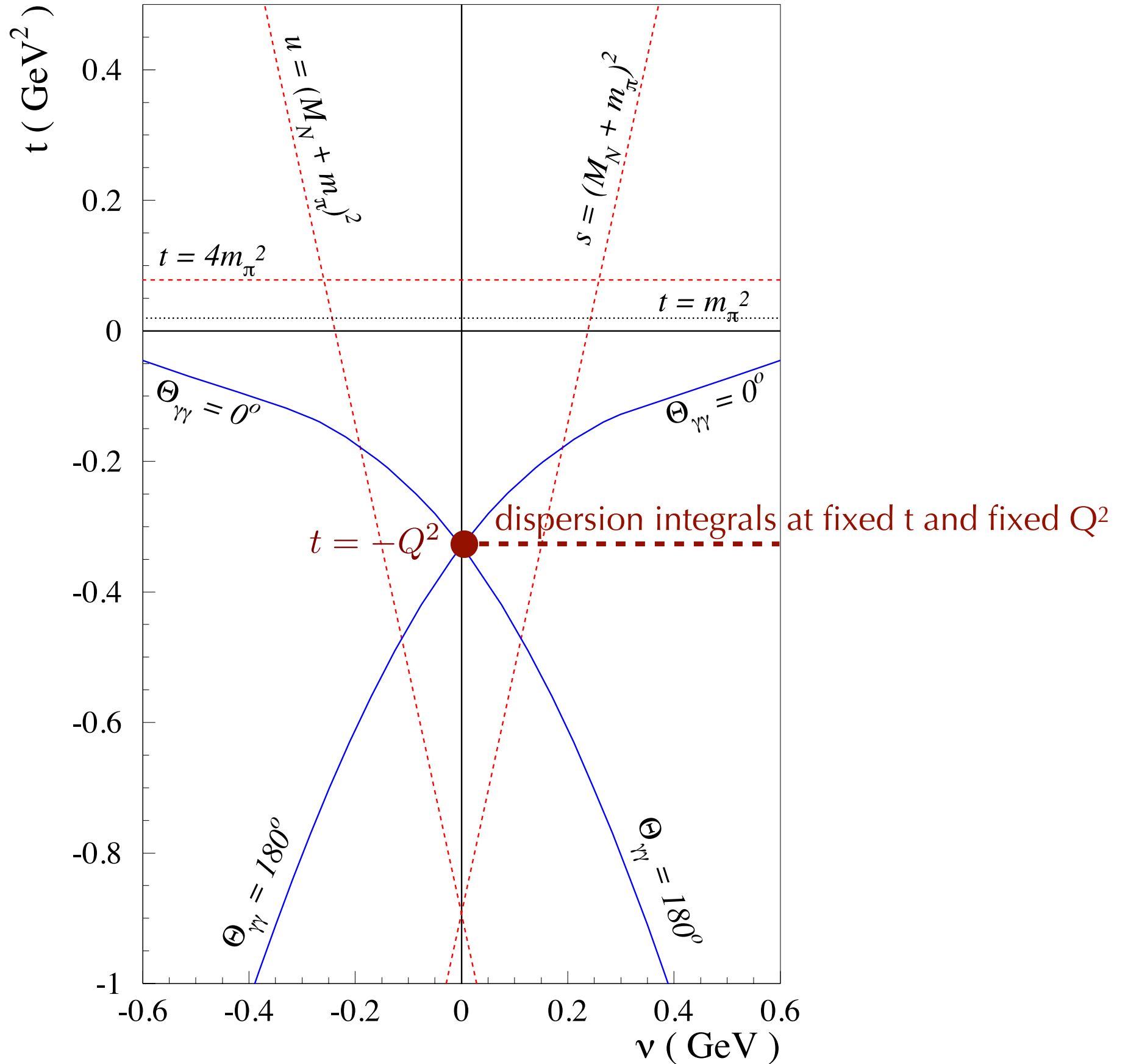
New data for scalar pol. from MAMI: A2 Coll. (MAMI), to appear in 2021 (PhD Thesis E. Mornacchi)



*Virtual scattering at threshold can be interpreted
as electron scattering by a target which is in constant electric and magnetic fields*



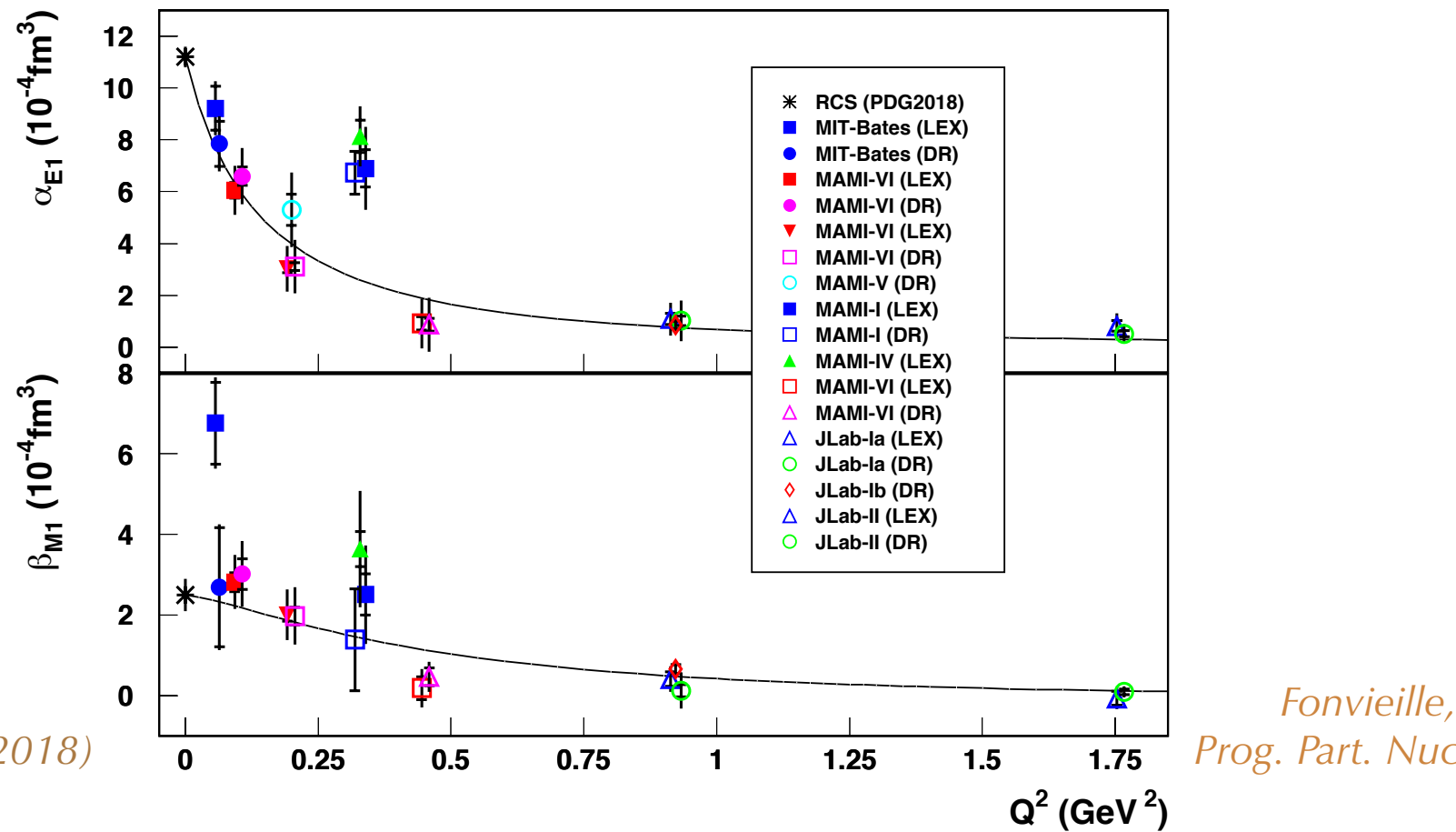
Mandelstam Plane for VCS at fixed Q^2



Status of VCS scalar polarizabilities

Unsubtracted DRs
fitted to data

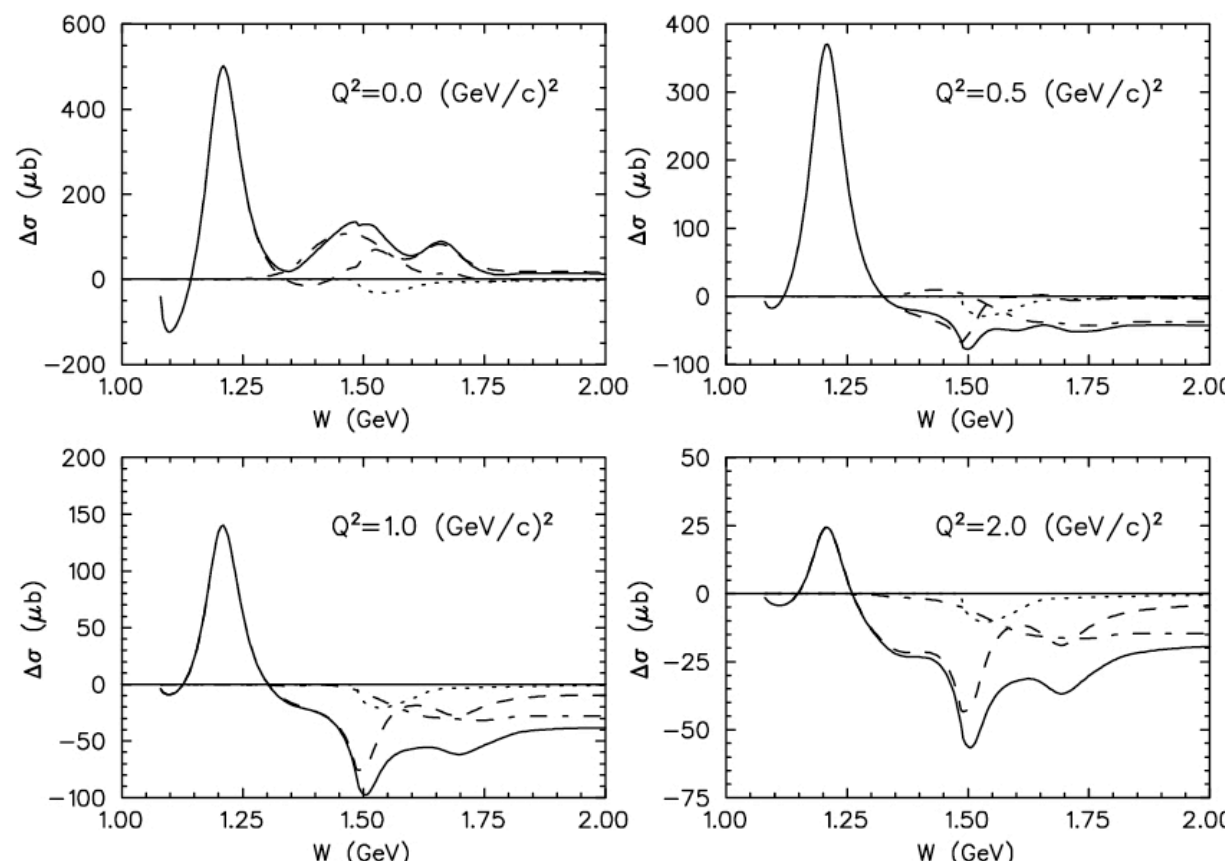
two-parameter fit



BP, Vanderhaeghen,
Ann. Rev. Nucl. Part. Sci. 68 (2018)

Fonvieille, BP, Sparveris,
Prog. Part. Nucl. Phys. 113 (2020)

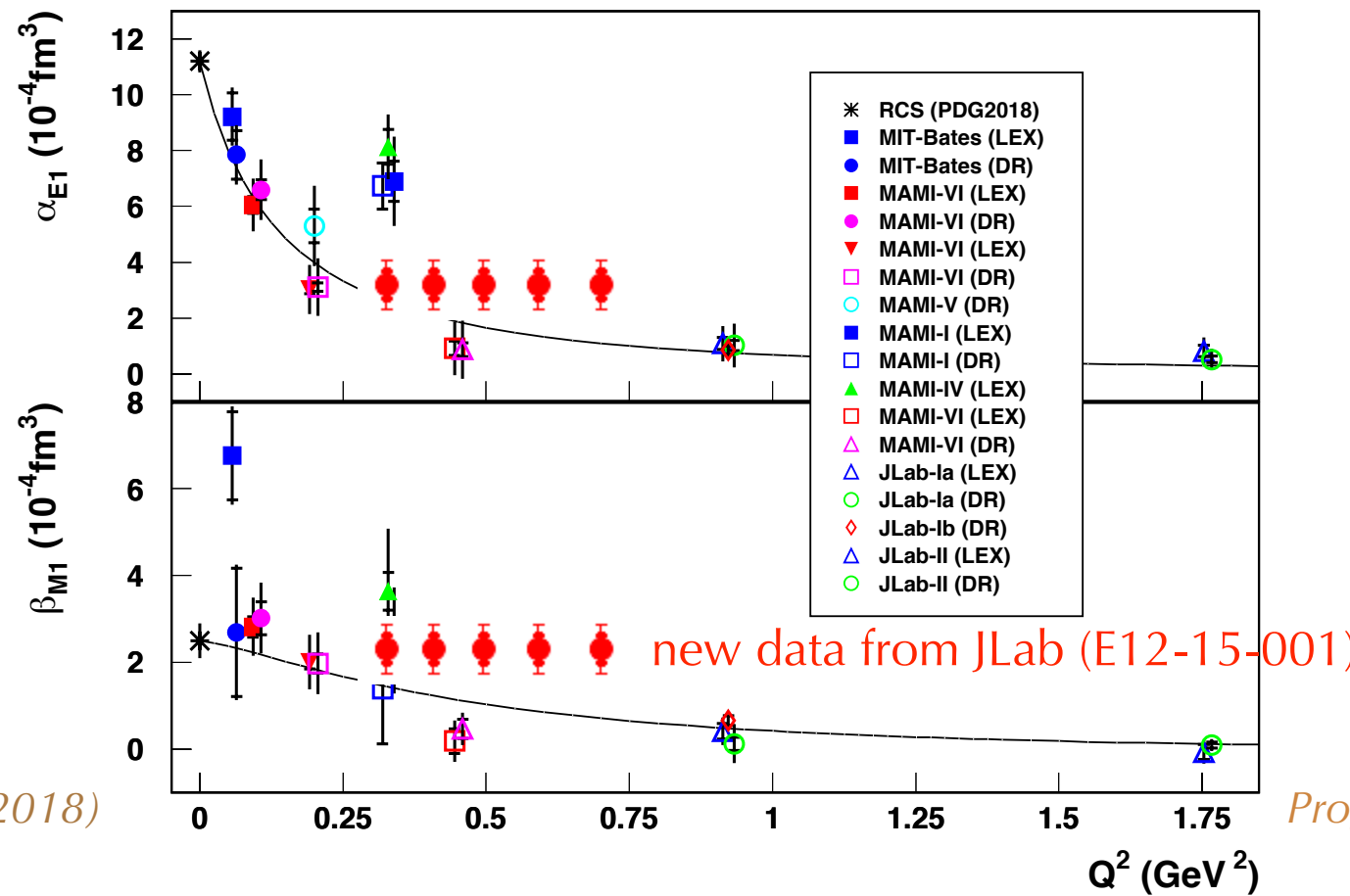
Input to dispersion integrals:
resonant and non-resonant
meson electroproduction amplitudes
and multi-meson electroproduction
amplitudes
-> probe the whole nucleon spectrum



Status of VCS scalar polarizabilities

Unsubtracted DRs
fitted to data

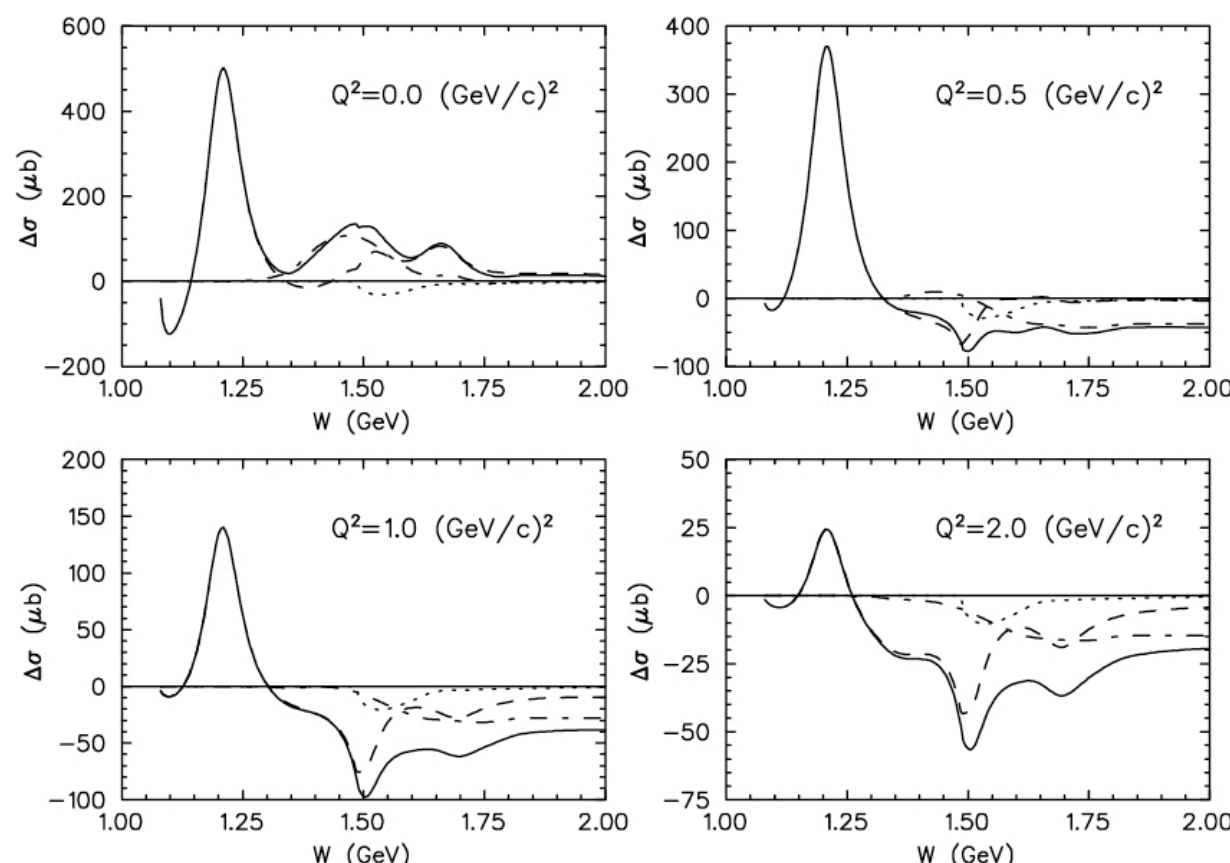
two-parameter fit



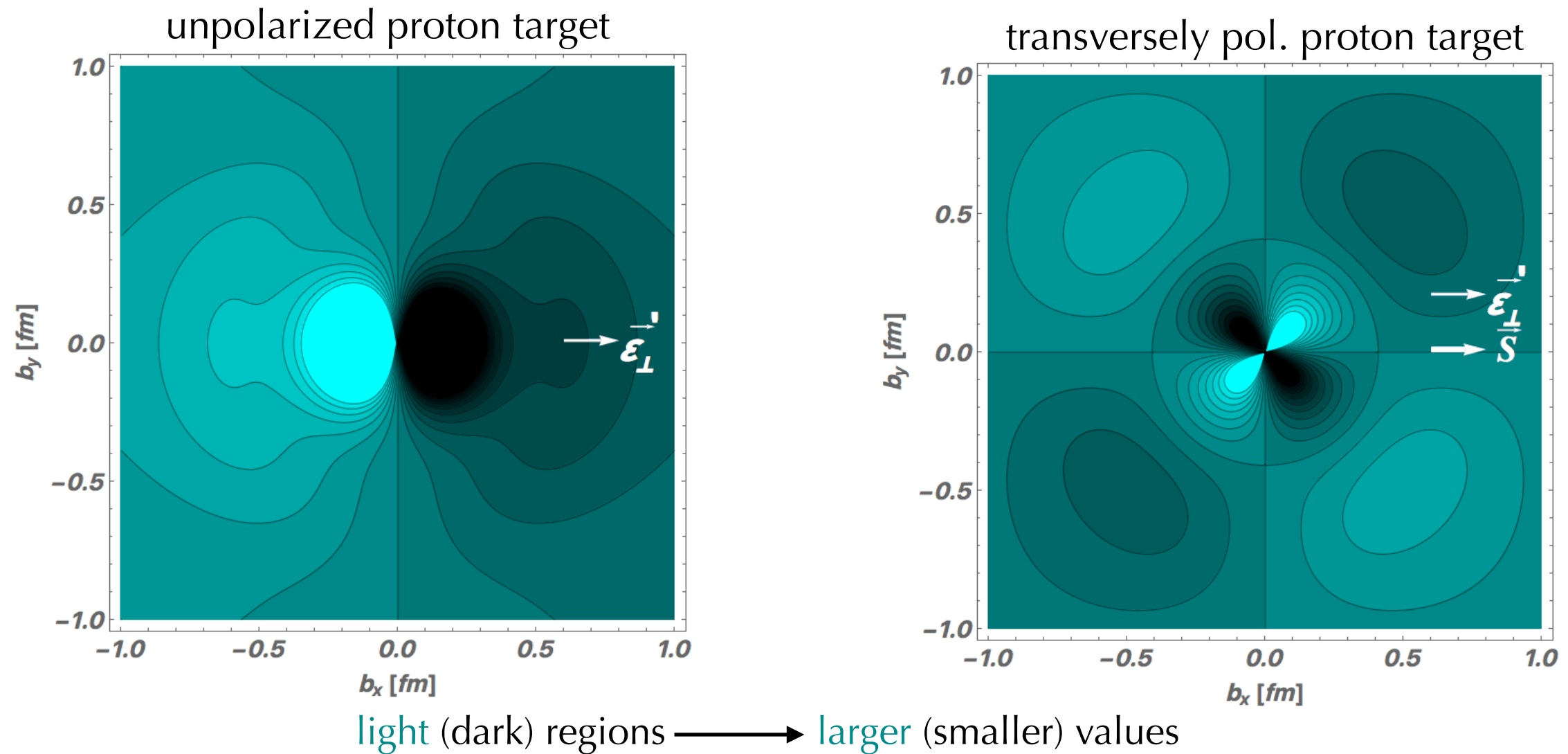
BP, Vanderhaeghen,
Ann. Rev. Nucl. Part. Sci. 68 (2018)

Fonvieille, BP, Sparveris,
Prog. Part. Nucl. Phys. 113 (2020)

Input to dispersion integrals:
resonant and non-resonant
meson electroproduction amplitudes
and multi-meson electroproduction
amplitudes
-> probe the whole nucleon spectrum



Spatial density of induced polarizations

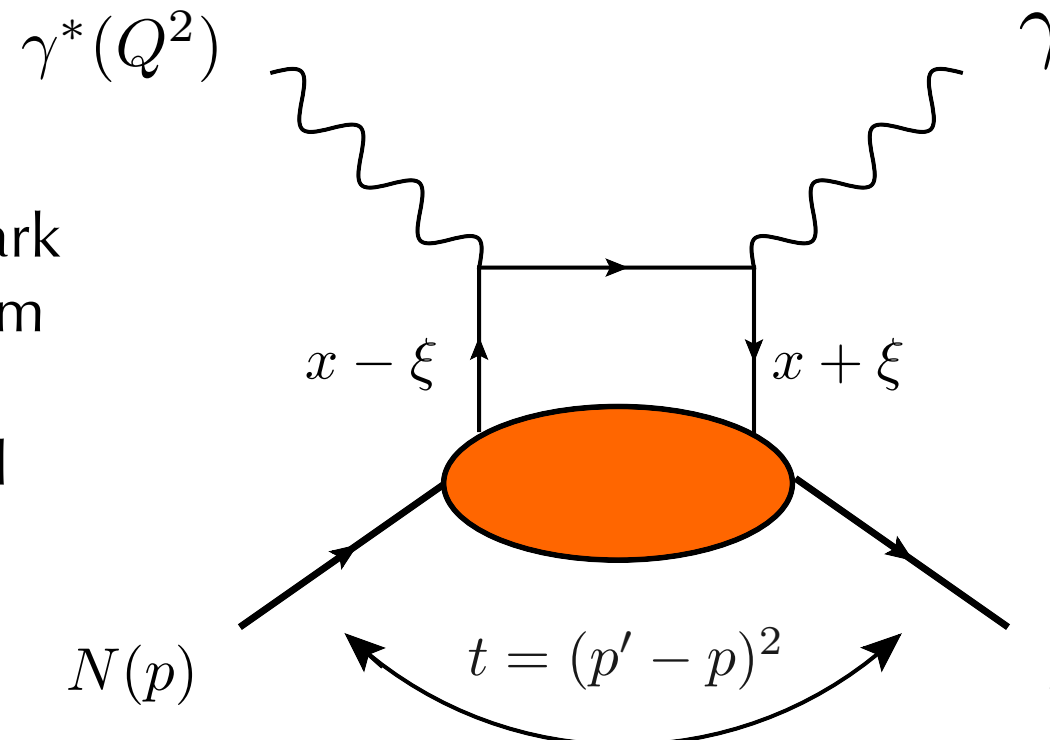


Frame with fast moving proton
in the longitudinal direction and $Q^2 = q_\perp^2$

$$\vec{q}_\perp \xleftrightarrow{\text{FT}} \vec{b}_\perp \quad \text{true probabilistic interpretation!}$$

$\vec{E} \sim iq'^0 \vec{\epsilon}'_\perp$ quasi-static electric field → \vec{P} induced polarization depending
on scalar and spin GPs

DVCS at leading twist



x : average fraction of quark longitudinal momentum

ξ : fraction of longitudinal momentum transfer

t : nucleon momentum transfer

DVCS tensor at twist 2:

$$T^{\mu\nu} = \sum_{i=1}^4 A_i(\nu, t, Q^2) O_i^{\mu\nu}$$

unpolarized quark

$$A_1 = \mathcal{H} + \mathcal{E}$$

$$A_2 = \mathcal{E}$$

Compton form factors: $\mathcal{F} = \int_0^1 dx F^+(x, \xi, t, Q^2) \left[\frac{1}{x - \xi + i\epsilon} + \frac{1}{x + \xi - i\epsilon} \right]$

$F = \{H, E, \tilde{H}, \tilde{E}\}$

↓

singlet GPDs: $F^+(x, \xi, t) = F(x, \xi, t) - F(-x, \xi, t)$

$$t \ll \nu, Q^2$$

↓

crossing symmetric variable

$$\nu = \frac{s - u}{4M_N}$$

long. polarized quark

$$A_3 = \tilde{\mathcal{H}}$$

$$A_4 = \tilde{\mathcal{E}}$$

Form Factors of Energy Momentum Tensor

| | Energy Density | Momentum Density | | |
|-------------|----------------|------------------|----------|----------|
| | T^{00} | T^{01} | T^{02} | T^{03} |
| | T^{10} | T^{11} | T^{12} | T^{13} |
| | T^{20} | T^{21} | T^{22} | T^{23} |
| | T^{30} | T^{31} | T^{32} | T^{33} |
| Energy Flux | | Momentum Flux | | |

shear forces

pressure

$$\langle p | T_{\mu\nu}^{Q,G} | p' \rangle = \bar{u}(p') \left[M_2^{Q,G}(t) \frac{P_\mu P_\nu}{M_N} + J^{Q,G}(t) \frac{i(P_\mu \sigma_{\nu\rho} + P_\nu \sigma_{\mu\rho}) \Delta^\rho}{2M_N} + d_1^{Q,G}(t) \frac{\Delta_\mu \Delta_\nu - g_{\mu\nu} \Delta^2}{5M_N} \pm \bar{c}(t) g_{\mu\nu} \right] u(p)$$

Relation with second-moments of GPDs:

“Charges” of the EMT Form Factors at t=0

$$\sum_q \int dx x H^q(x, \xi, t) = M_2^Q(t) + \frac{4}{5} d_1^Q(t) \xi^2$$

$M_2(0)$ nucleon momentum carried by parton

$J(0)$ angular momentum of partons

$$\sum_q \int dx x E^q(x, \xi, t) = 2J^Q(t) - M_2^Q(t) - \frac{4}{5} d_1^Q(t) \xi^2$$

$d_1(0)$ D-term (“stability” of the nucleon)

Form Factors of Energy Momentum Tensor

| | Energy Density | Momentum Density | | |
|--|----------------|------------------|----------|----------|
| | T^{00} | T^{01} | T^{02} | T^{03} |
| | T^{10} | T^{11} | T^{12} | T^{13} |
| | T^{20} | T^{21} | T^{22} | T^{23} |
| | T^{30} | T^{31} | T^{32} | T^{33} |

Energy Flux Momentum Flux

shear forces

pressure

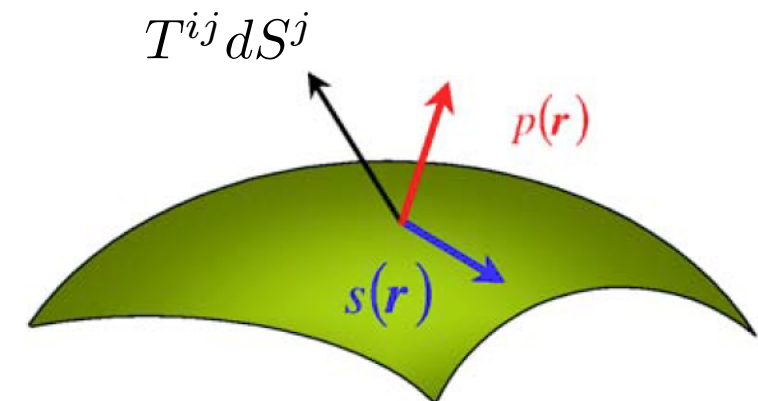
→ Fourier transform in coordinate space

$$T_{ij}^Q(\vec{r}) = s(\vec{r}) \left(\frac{r_i r_j}{r^2} - \frac{1}{3} \delta_{ij} \right) + p(\vec{r}) \delta_{ij}$$

↓
shear forces ↓
pressure

$$d_1^Q(0) = 5\pi M_N \int_0^\infty dr r^4 p(r)$$

“mechanical properties” of nucleon



Dispersion Relations for DVCS amplitudes

- s-channel subtracted DRs:

$$\text{Re } A_2(\nu, t, Q^2) = \Delta(t, Q^2) + \frac{2}{\pi} \nu^2 \mathcal{P} \int_{\nu_0}^{\infty} \text{Im } A_2(\nu', t, Q^2) \frac{d\nu'}{\nu'(\nu'^2 - \nu^2)}$$

Dispersion Relations for DVCS amplitudes

- s-channel subtracted DRs:

$$\text{Re } A_2(\nu, t, Q^2) = \Delta(t, Q^2) + \frac{2}{\pi} \nu^2 \mathcal{P} \int_{\nu_0}^{\infty} \text{Im } A_2(\nu', t, Q^2) \frac{d\nu'}{\nu'(\nu'^2 - \nu^2)}$$

- t-channel DRs for subtraction function

$$\Delta(t, Q^2) = -\frac{4}{N_f} D(t, Q^2) = \frac{1}{\pi} \int_{4m_\pi^2}^{\infty} dt' \frac{\text{Im}_t A_2(0, t', Q^2)}{t' - t} + \frac{1}{\pi} \int_{-\infty}^{-a} dt' \frac{\text{Im}_t A_2(0, t', Q^2)}{t' - t}$$

↓

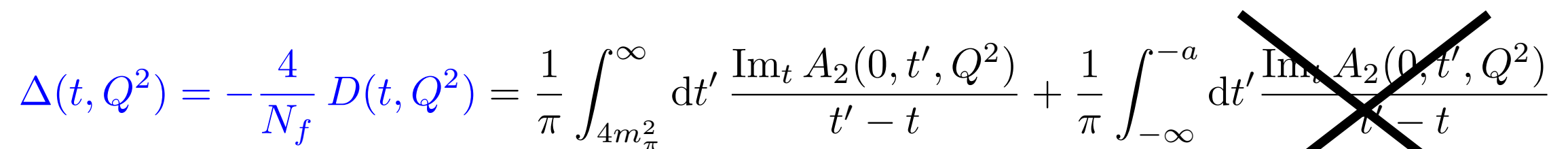
$$-a = -2(m_\pi^2 + 2M_N m_\pi) - Q^2$$

Dispersion Relations for DVCS amplitudes

- s-channel subtracted DRs:

$$\text{Re } A_2(\nu, t, Q^2) = \Delta(t, Q^2) + \frac{2}{\pi} \nu^2 \mathcal{P} \int_{\nu_0}^{\infty} \text{Im } A_2(\nu', t, Q^2) \frac{d\nu'}{\nu'(\nu'^2 - \nu^2)}$$

- t-channel DRs for subtraction function

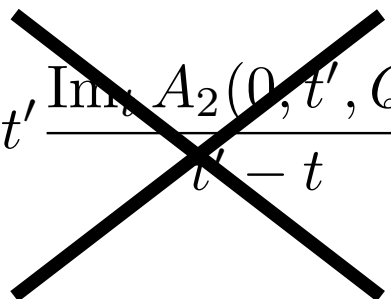
$$\Delta(t, Q^2) = -\frac{4}{N_f} D(t, Q^2) = \frac{1}{\pi} \int_{4m_\pi^2}^{\infty} dt' \frac{\text{Im}_t A_2(0, t', Q^2)}{t' - t} + \frac{1}{\pi} \int_{-\infty}^{-a} dt' \frac{\text{Im}_t A_2(0, t', Q^2)}{t' - t}$$


Dispersion Relations for DVCS amplitudes

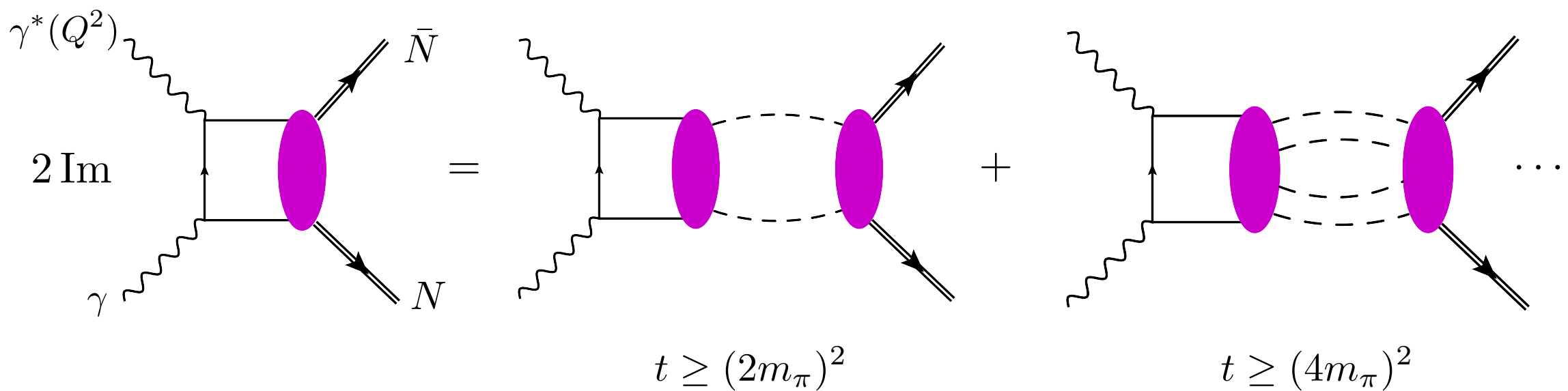
- s-channel subtracted DRs:

$$\text{Re } A_2(\nu, t, Q^2) = \Delta(t, Q^2) + \frac{2}{\pi} \nu^2 \mathcal{P} \int_{\nu_0}^{\infty} \text{Im } A_2(\nu', t, Q^2) \frac{d\nu'}{\nu'(\nu'^2 - \nu^2)}$$

- t-channel DRs for subtraction function

$$\Delta(t, Q^2) = -\frac{4}{N_f} D(t, Q^2) = \frac{1}{\pi} \int_{4m_\pi^2}^{\infty} dt' \frac{\text{Im}_t A_2(0, t', Q^2)}{t' - t} + \frac{1}{\pi} \int_{-\infty}^{-a} dt' \frac{\text{Im}_t A_2(0, t', Q^2)}{t' - t}$$


Unitarity relation in t-channel

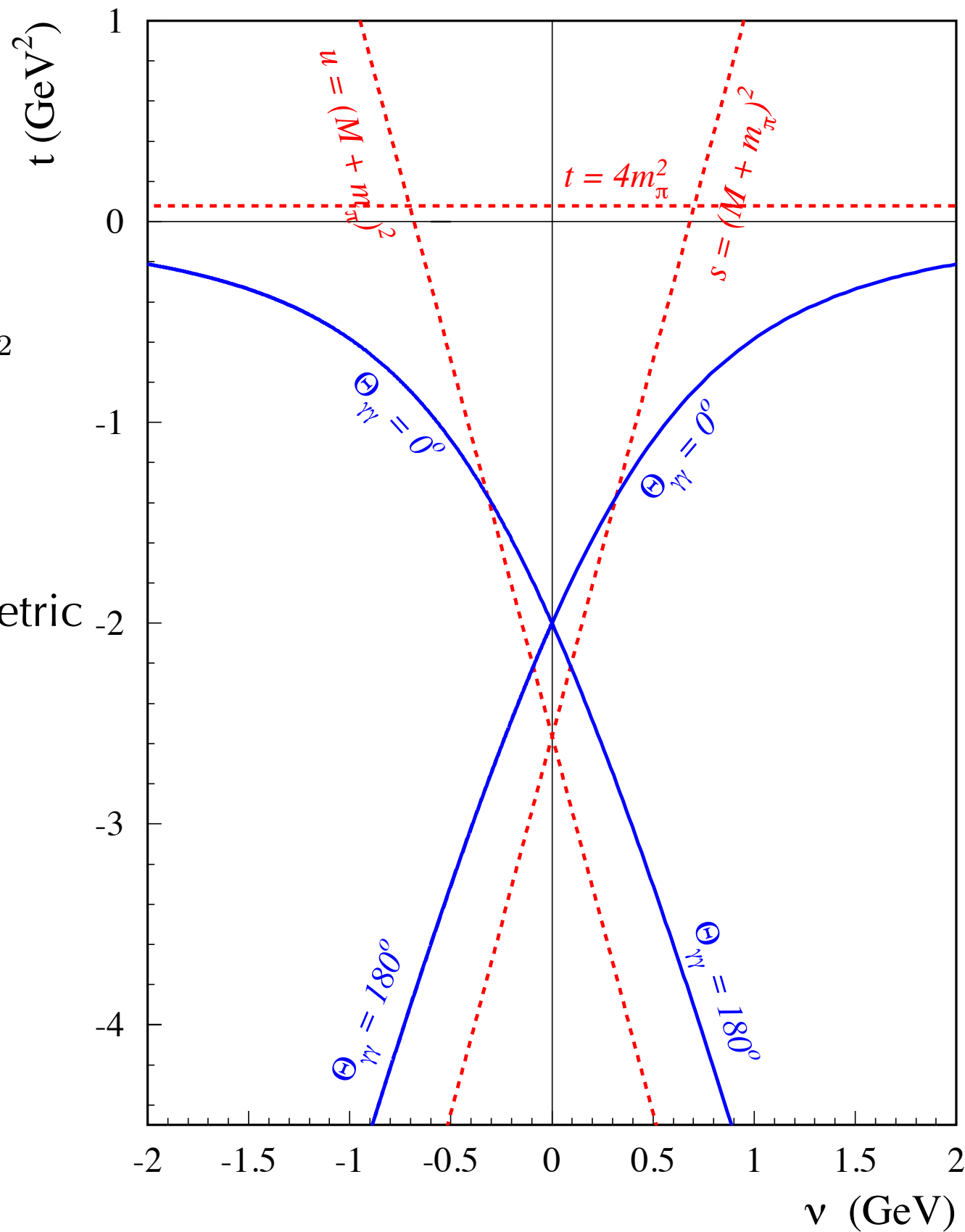


Fixed

$$Q^2 = -2 \text{ GeV}^2$$

$$\nu = \frac{s-u}{4M_N}$$

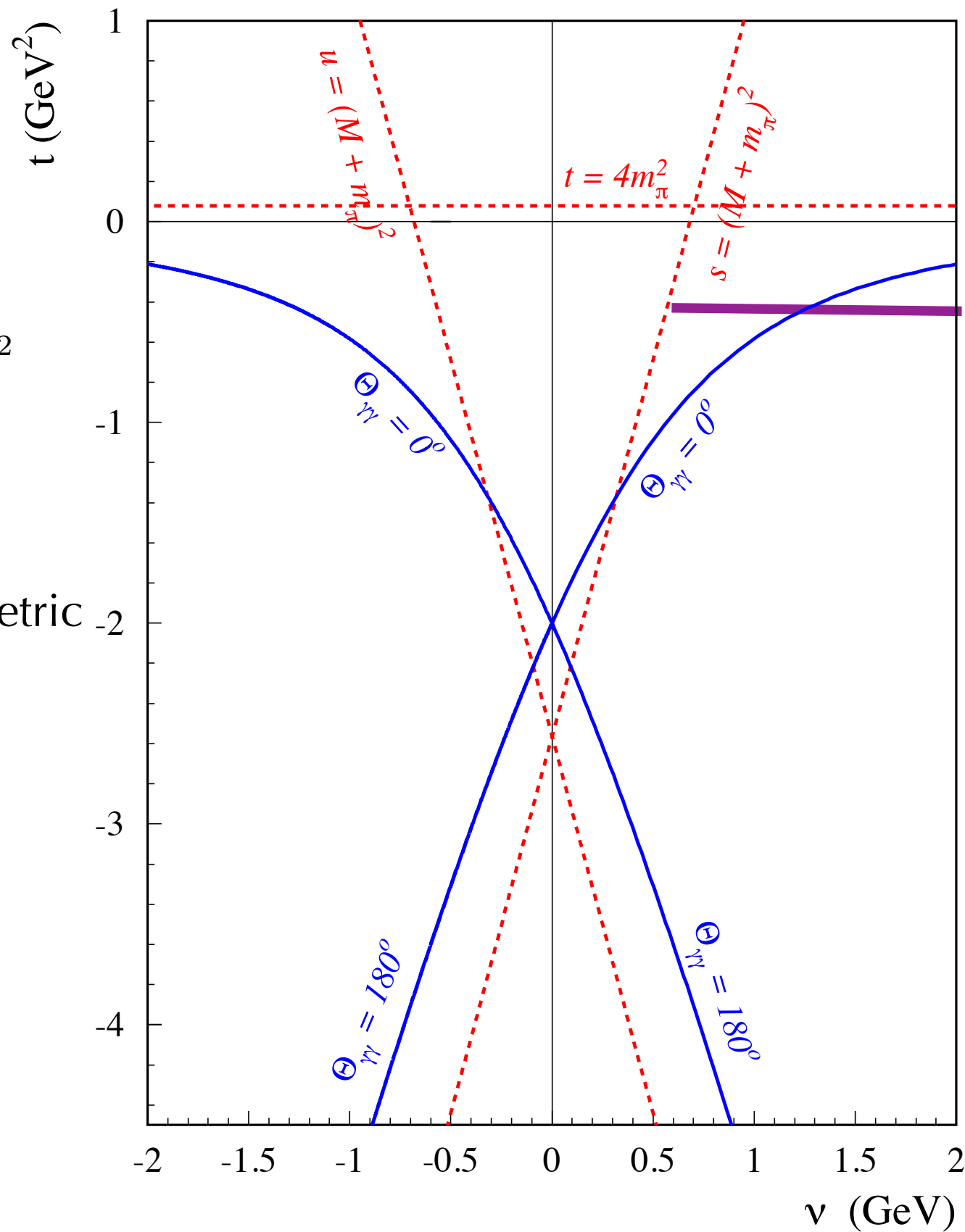
crossing symmetric variable



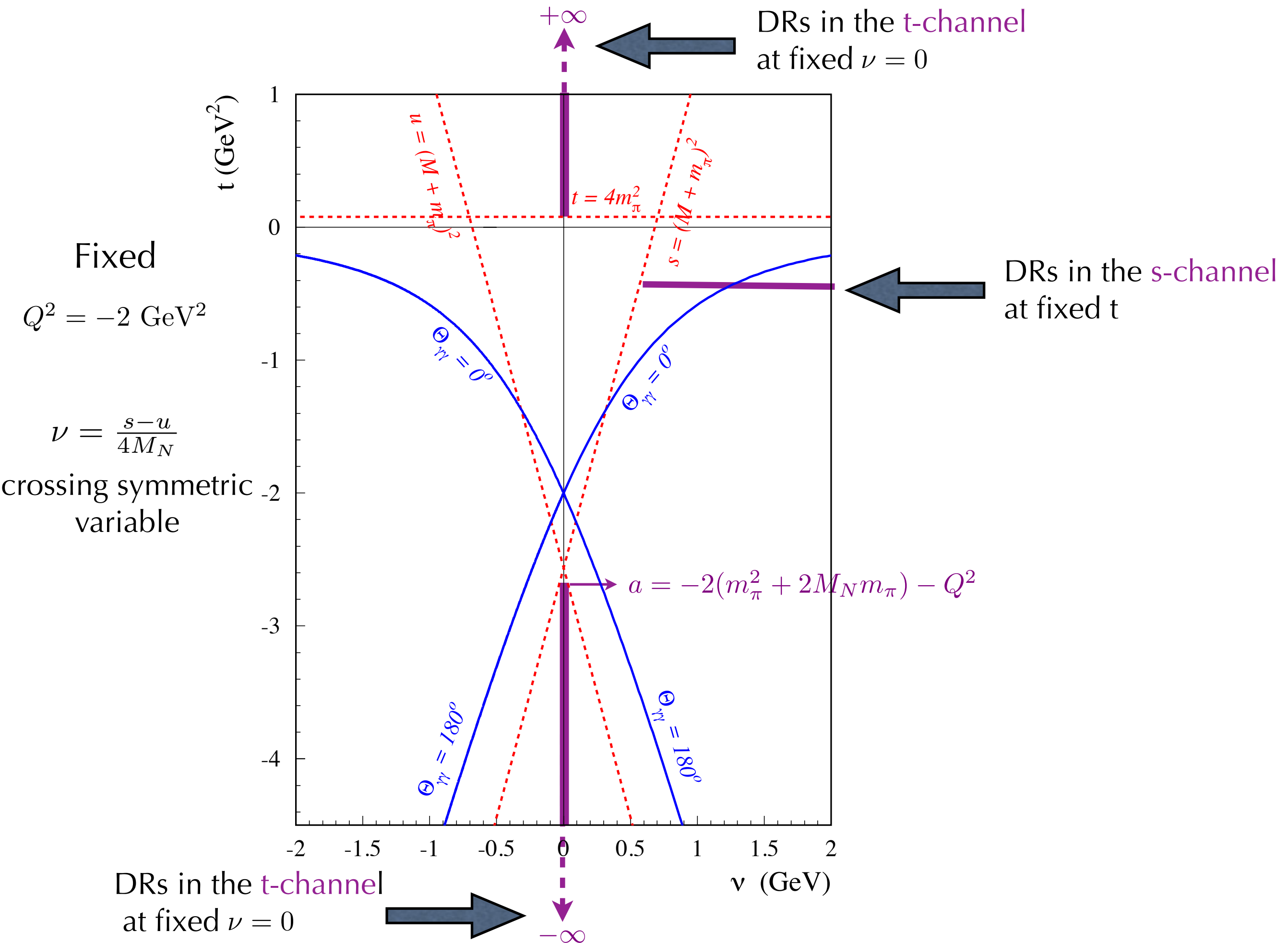
Fixed
 $Q^2 = -2 \text{ GeV}^2$

$$\nu = \frac{s-u}{4M_N}$$

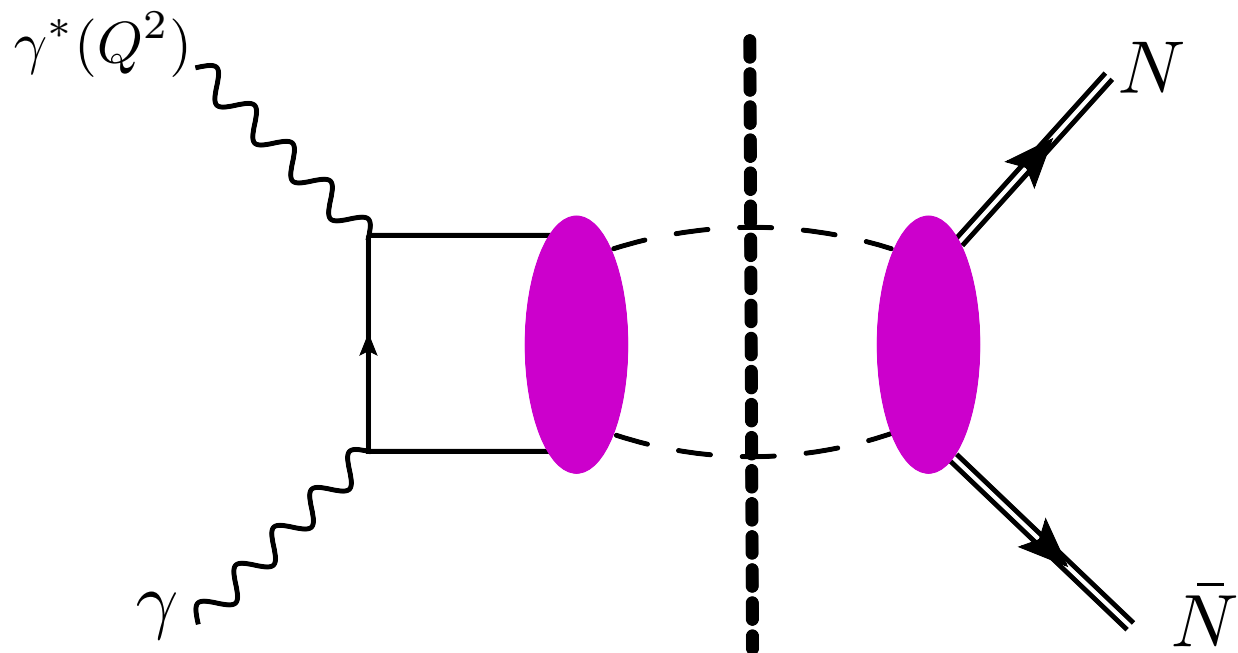
crossing symmetric variable



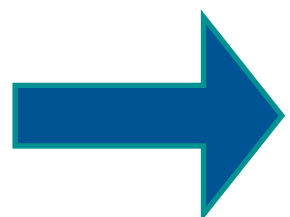
DRs in the *s*-channel
at fixed t



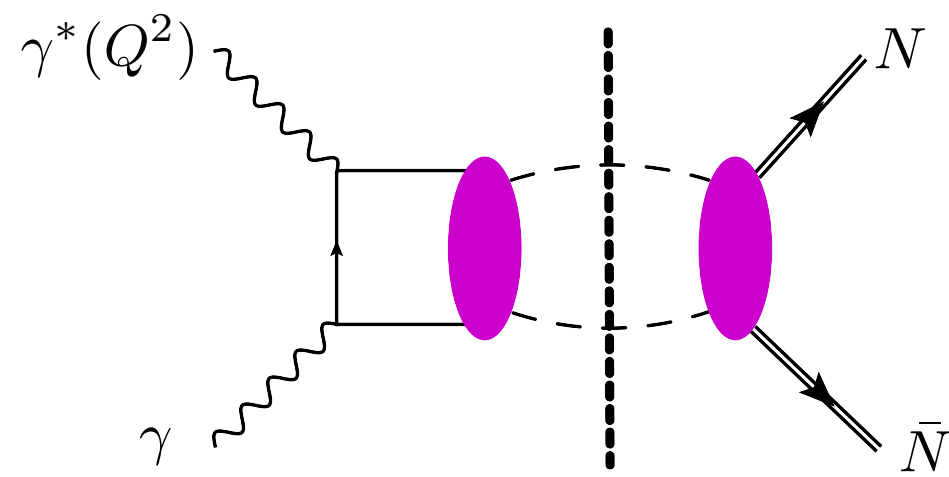
Unitarity Relations in the t-channel



- Charge conjugation
- Partial wave expansion
with $\nu = 0 \rightarrow \theta_t = 90^\circ$

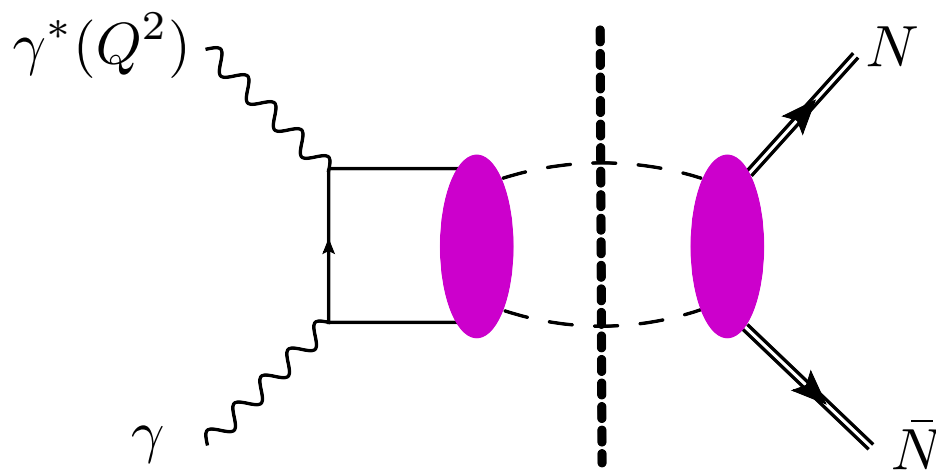


two-pion intermediate state with
 $I = 0 \quad J = 0, 2, \dots$



Two-pion intermediate states with $I = 0$ and $J = 0, 2$

$$D(t) = \sum_{\{n \text{ odd}\}} d_n(t) \longrightarrow \text{DRs for } d_1(t)$$



Two-pion intermediate states with $I = 0$ and $J = 0, 2$

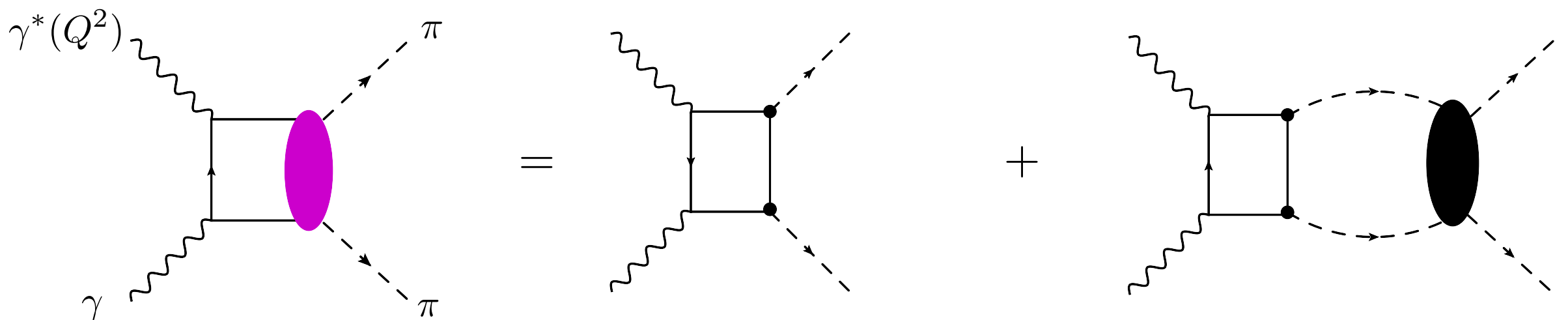
$$D(t) = \sum_{\{n \text{ odd}\}} d_n(t) \longrightarrow \text{DRs for } d_1(t)$$

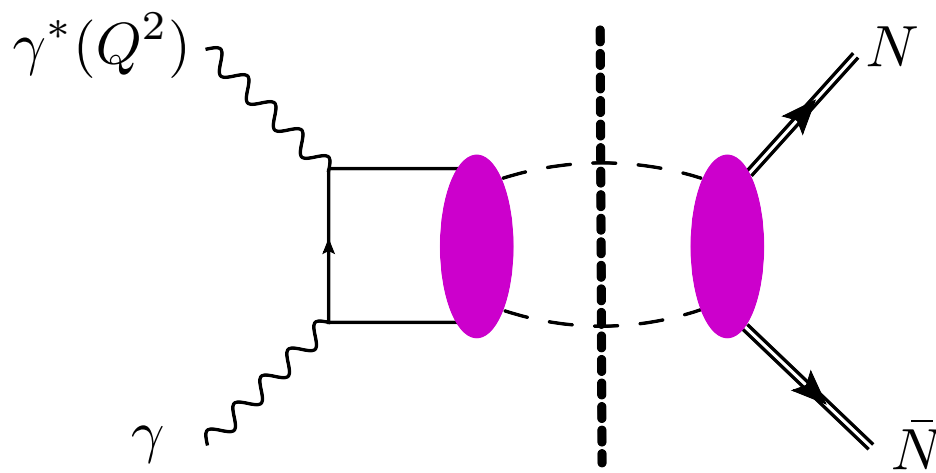
- $\gamma^* \gamma \rightarrow \pi\pi$: two-pion generalized distribution amplitudes \longrightarrow inputs

[

pion singlet PDF
 $\pi\pi$ phase-shifts

]

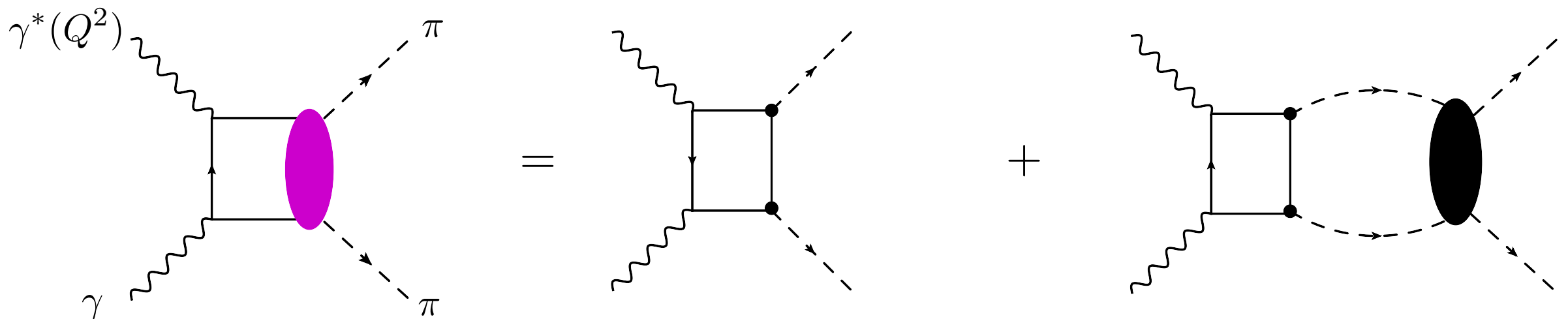




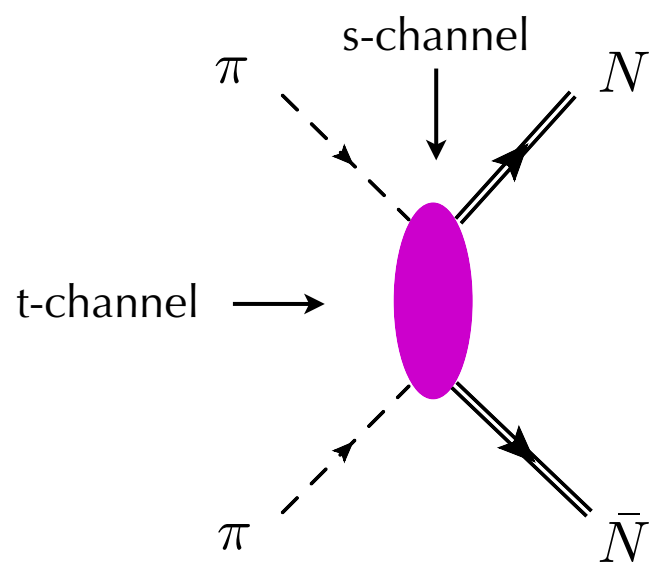
Two-pion intermediate states with $I = 0$ and $J = 0, 2$

$$D(t) = \sum_{\{n \text{ odd}\}} d_n(t) \longrightarrow \text{DRs for } d_1(t)$$

- $\gamma^* \gamma \rightarrow \pi\pi$: two-pion generalized distribution amplitudes \longrightarrow inputs $\begin{cases} \text{pion singlet PDF} \\ \pi\pi \text{ phase-shifts} \end{cases}$

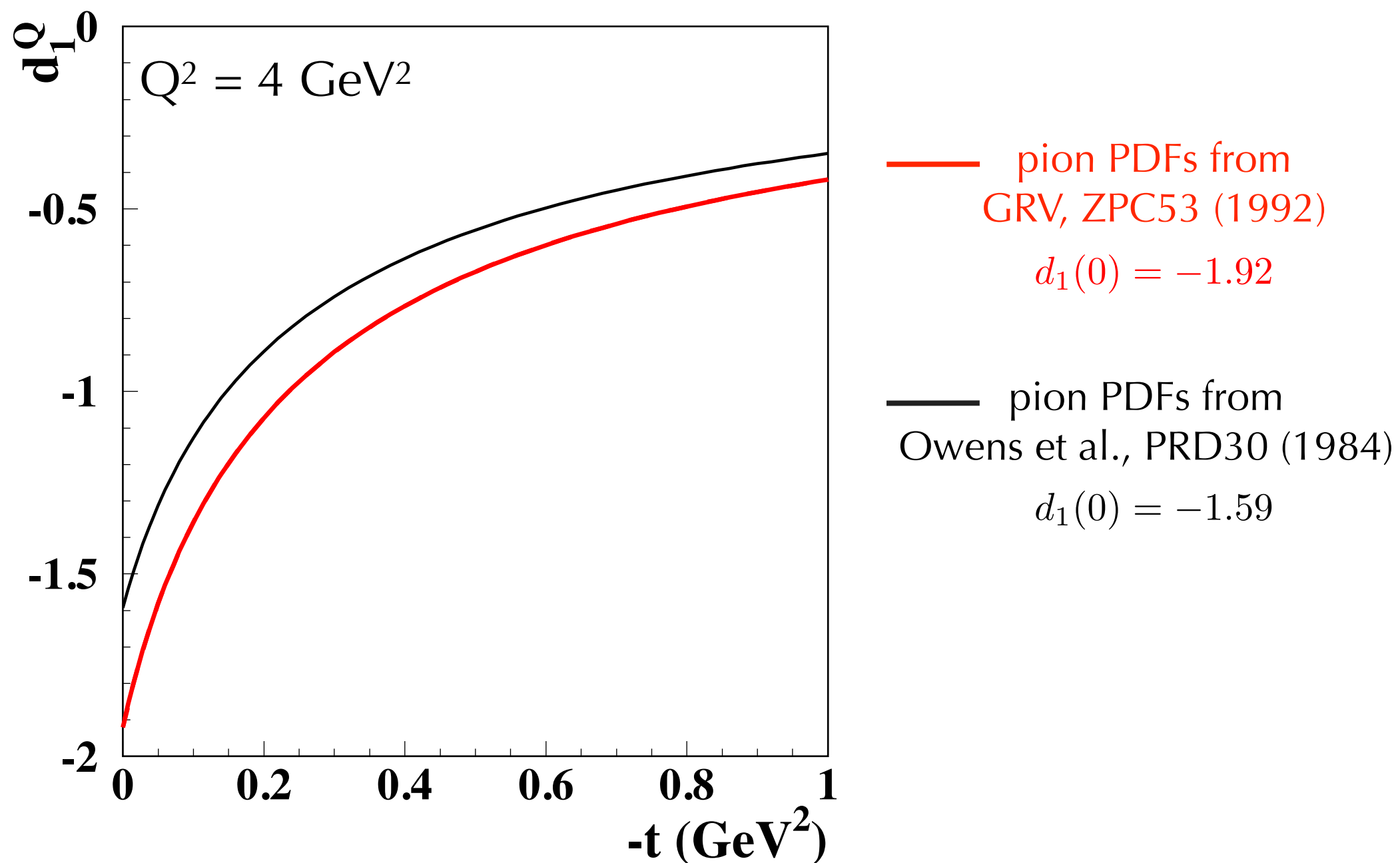


- $\pi\pi \rightarrow N\bar{N}$: analytical continuation of s-channel partial-wave helicity amplitudes \longrightarrow input $\pi\pi$ phase-shifts



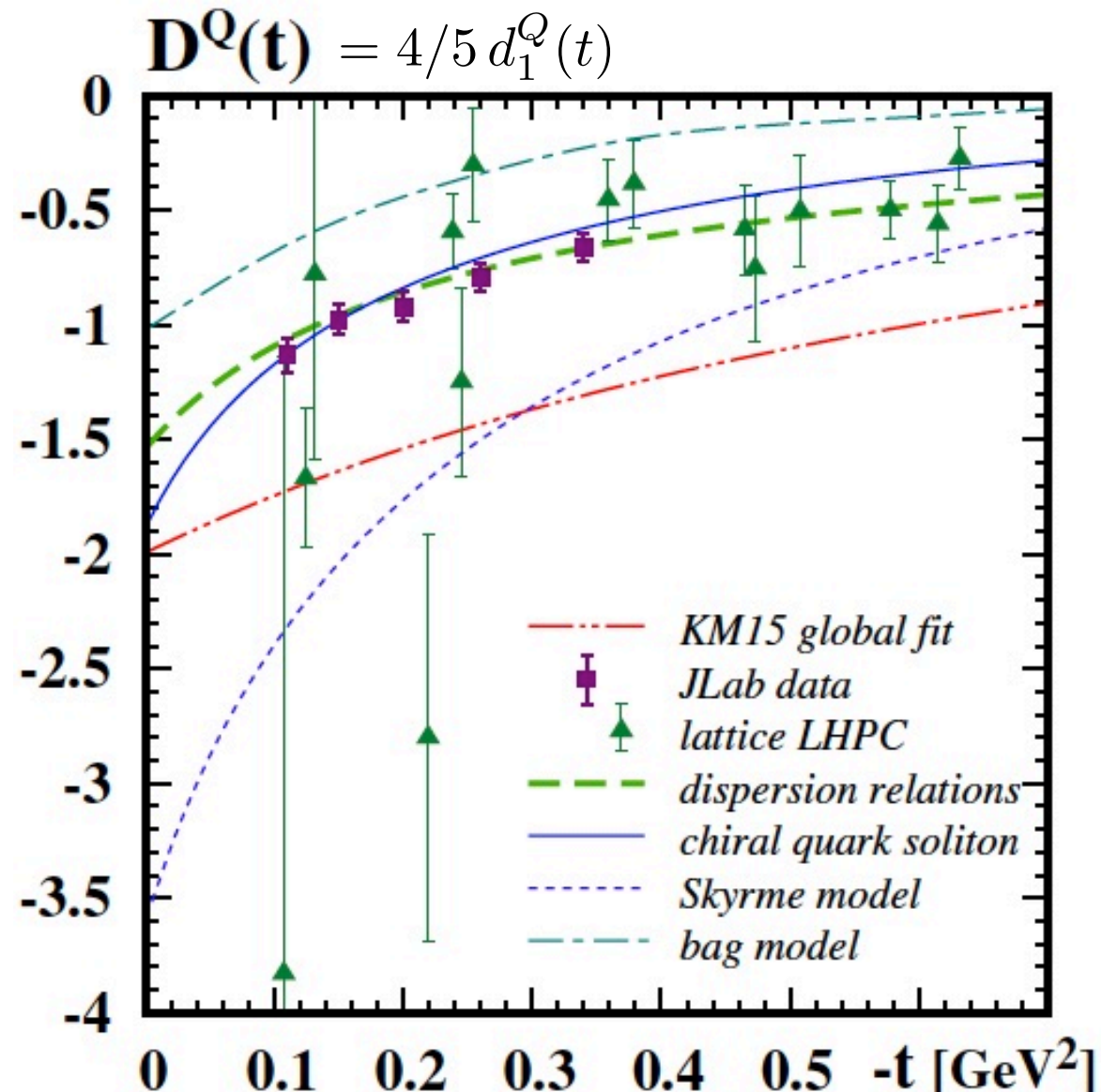
DR Results for D-term Form Factor

$Q = u + d$



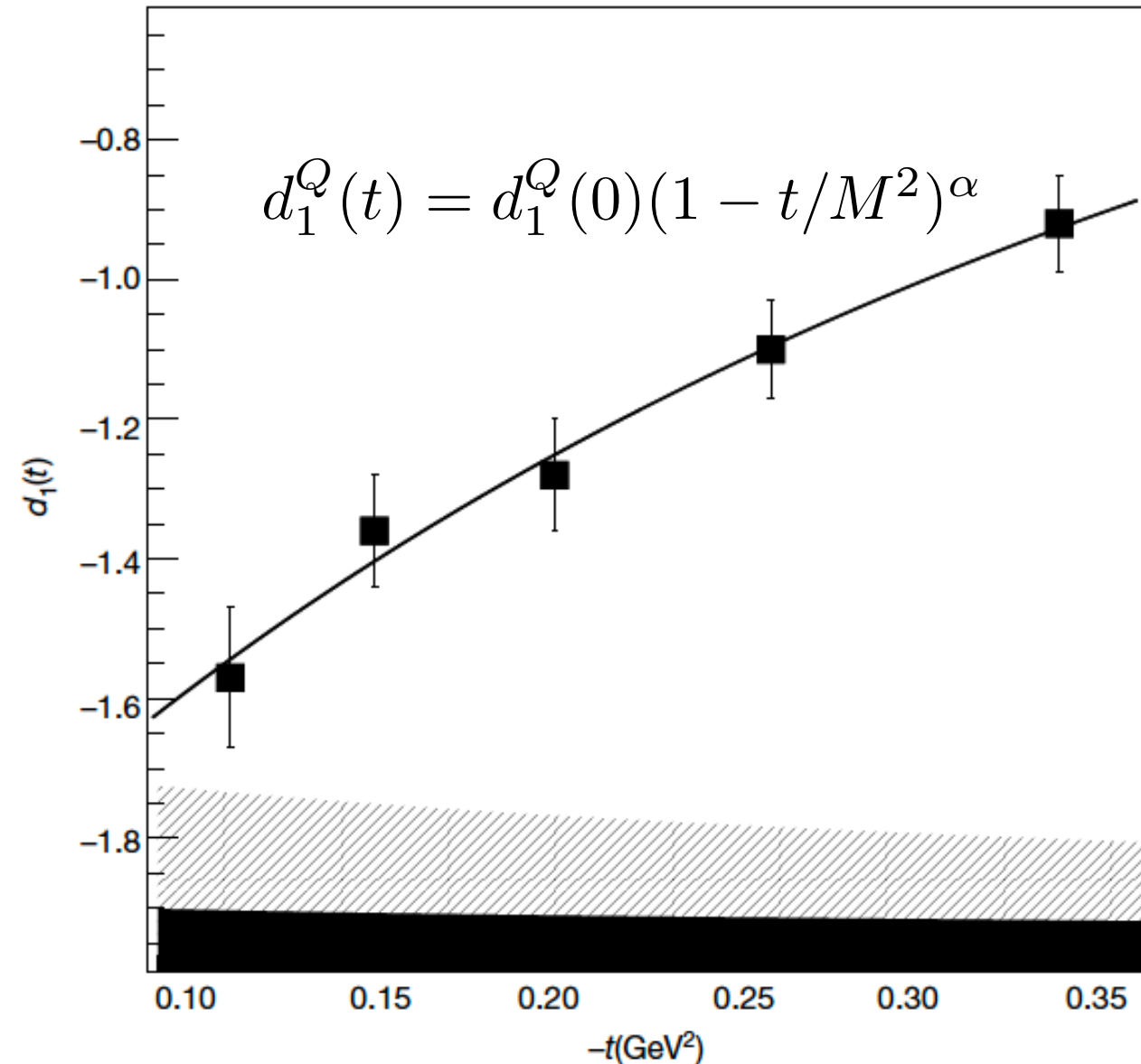
$D(t)$ form factor from data

Girod, Elouadrhiri, Burkert, Nature 557 (2018) 7705
and arXiv: 2104.02031;
CLAS 6GeV data



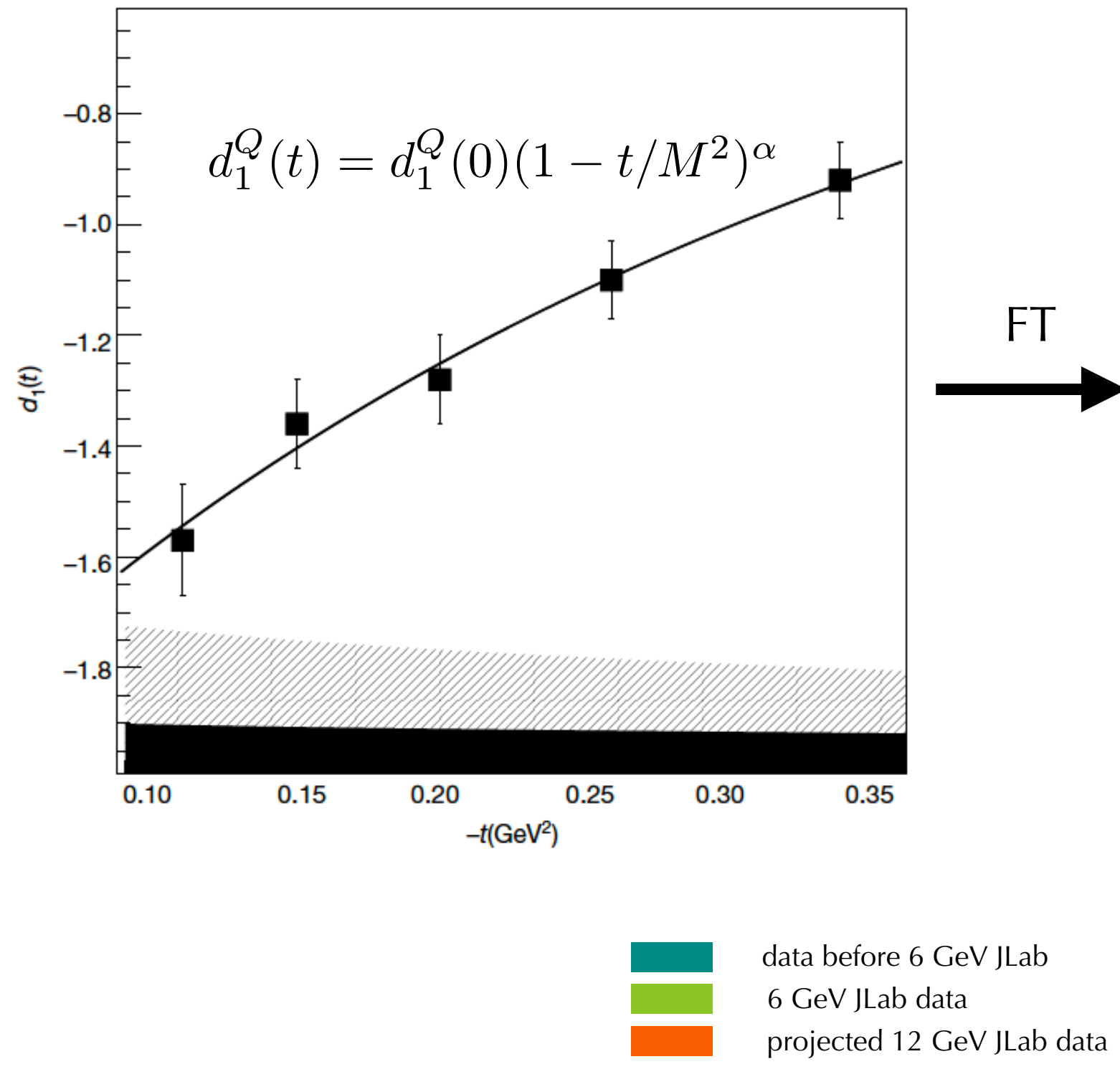
D(t) form factor from data

Girod, Elouadrhiri, Burkert, Nature 557 (2018) 7705
and arXiv: 2104.02031;
CLAS 6GeV data

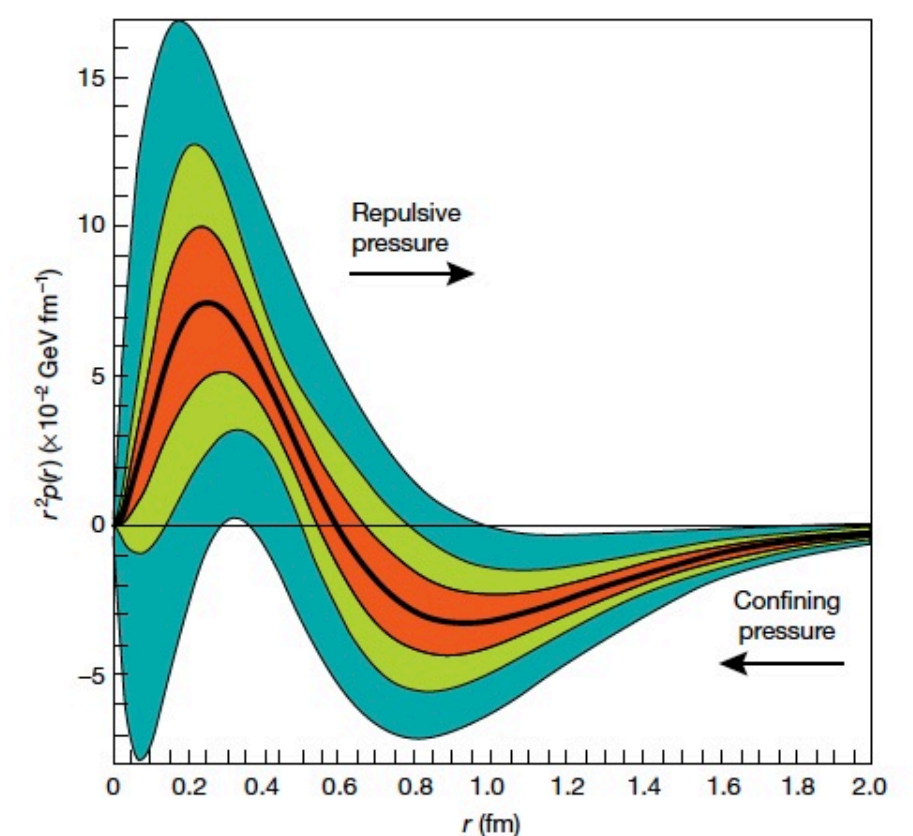


D(t) form factor from data

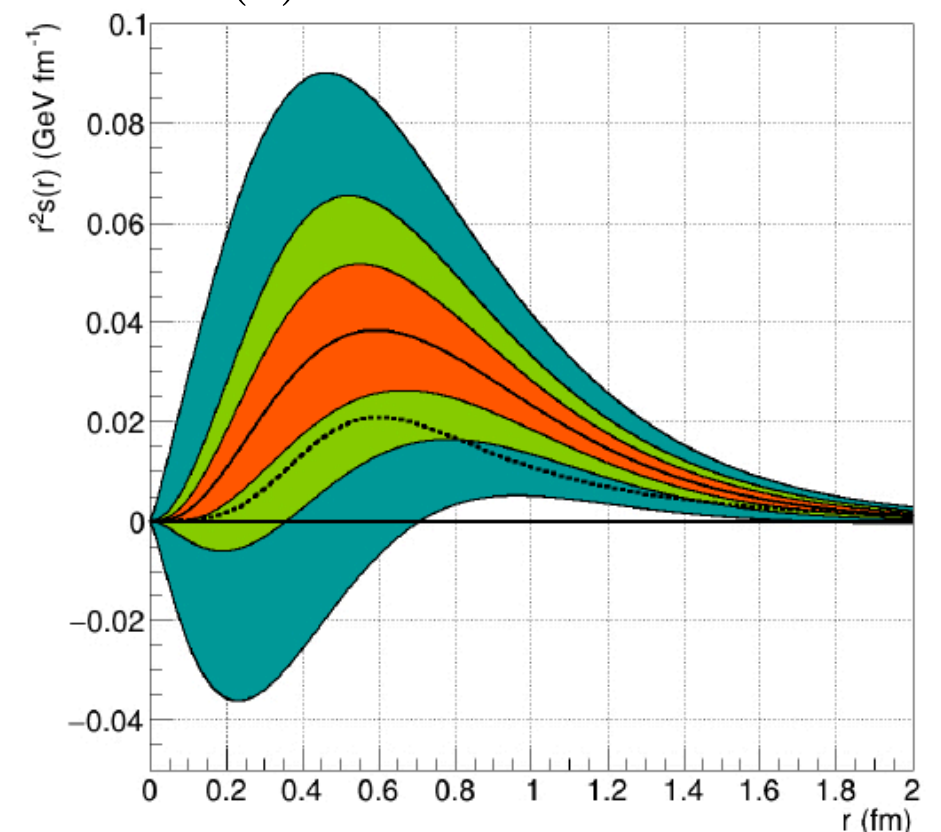
Girod, Elouadrhiri, Burkert, *Nature* 557 (2018) 7705
and arXiv: 2104.02031;
CLAS 6GeV data



$r^2 p(r)$ radial pressure distribution



$r^2 s(r)$ shear forces distribution

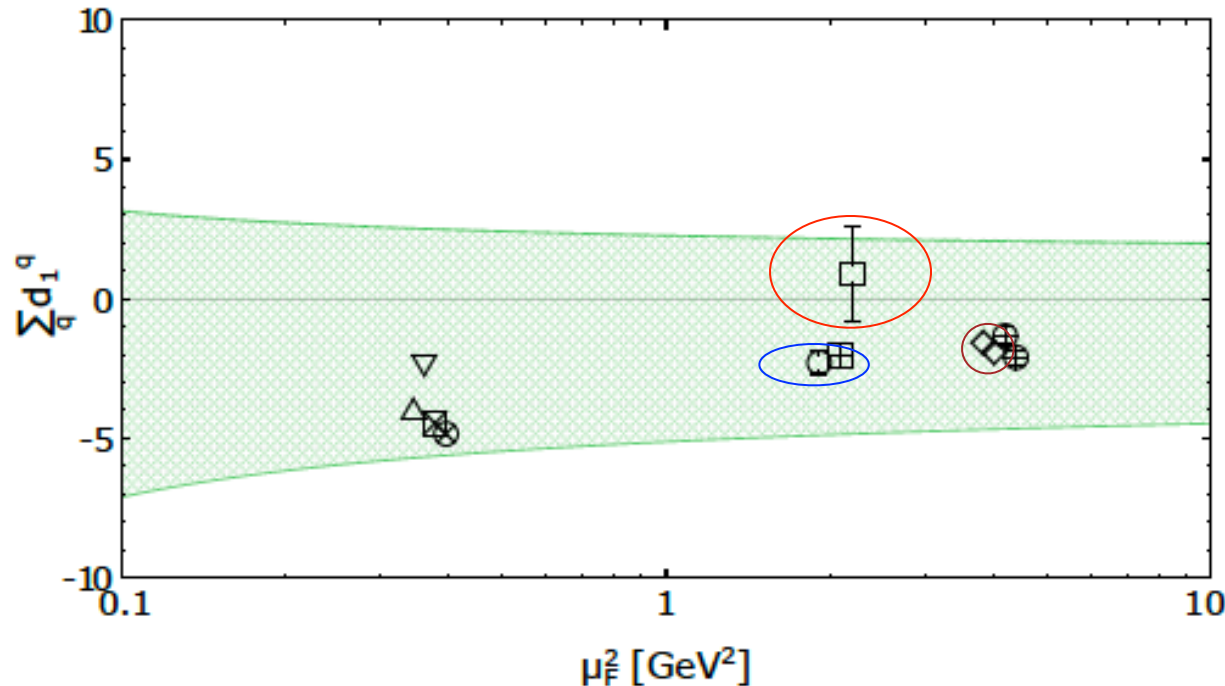


Necessary to verify model assumptions in the exp extraction
with more data coming from JLab, COMPASS and the future EIC, ElcC

Kumericki, Nature 570 (2019) 7759; Dutriex et al, arXiv: 2101.03855



global fit to DVCS data
with artificial neural networks



$\sum_q d_1^q < 0$
in all model calculations
for a stable proton

CLAS data, with fixed param.,
Girod et al.

CLAS data, with neural networks
Kumericki

| Marker in Fig. 3 | $\sum_q d_1^q(\mu_F^2)$ | μ_F^2 in GeV^2 | # of flavours | Type |
|---------------------|--------------------------------------|--------------------------------|------------------|--|
| (○) | $-2.30 \pm 0.16 \pm 0.37$ | 2.0 | 3 | from experimental data |
| (□) | 0.88 ± 1.69 | 2.2 | 2 | from experimental data |
| ◊ | -1.59 -1.92 | 4 4 | 2 2 | t-channel DRs |
| △ | -4 | 0.36 | 3 | χ QSM |
| ▽ | -2.35 | 0.36 | 2 | χ QSM |
| ⊗ | -4.48 | 0.36 | 2 | Skyrme model |
| 田 | -2.02 | 2 | 3 | LFWF model |
| ⊗ | -4.85 | 0.36 | 2 | χ QSM |
| ⊕ | -1.34 ± 0.31 -2.11 ± 0.27 | 4 4 | 2 2 | lattice QCD ($\overline{\text{MS}}$) lattice QCD ($\overline{\text{MS}}$) |

Dispersion Relations for Compton Scattering

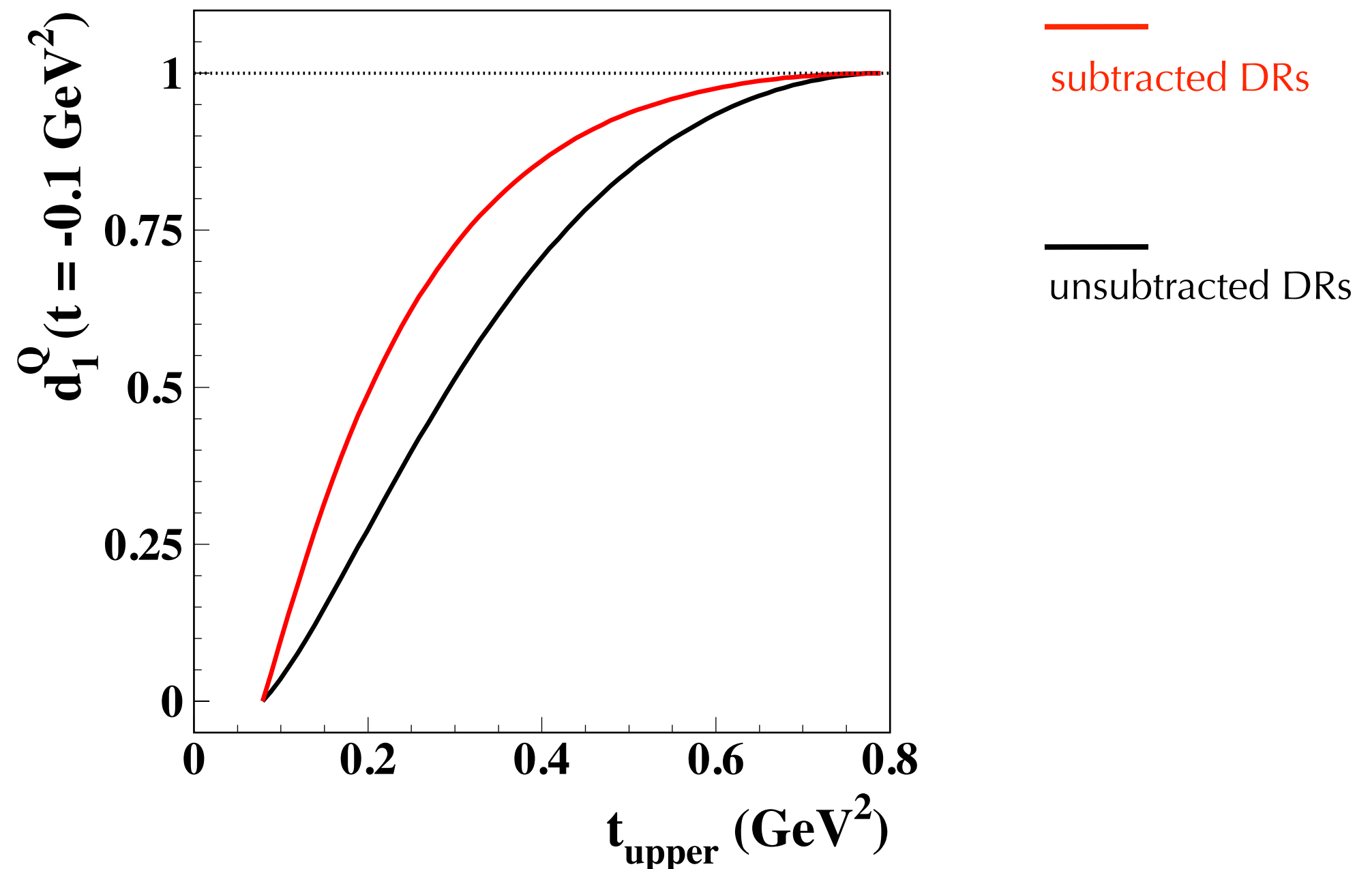
use available information from other channels to constrain nucleon e.m. structure with a minimum of model dependence

Future of Compton Scattering

- Improve accuracy in the extraction of the RCS polarizabilities
 - new upcoming data from MAMI with unprecedented precision
- Constrain the Q^2 dependence of the generalized polarizabilities
 - ongoing analysis of VCS data from JLab
- Big impact on GPD studies from JLab12, COMPASS, and future EIC
- New results for the VVCS polarizabilities from JLab
 - challenge for the theoretical interpretation

Backup Slides

Convergence of DRs



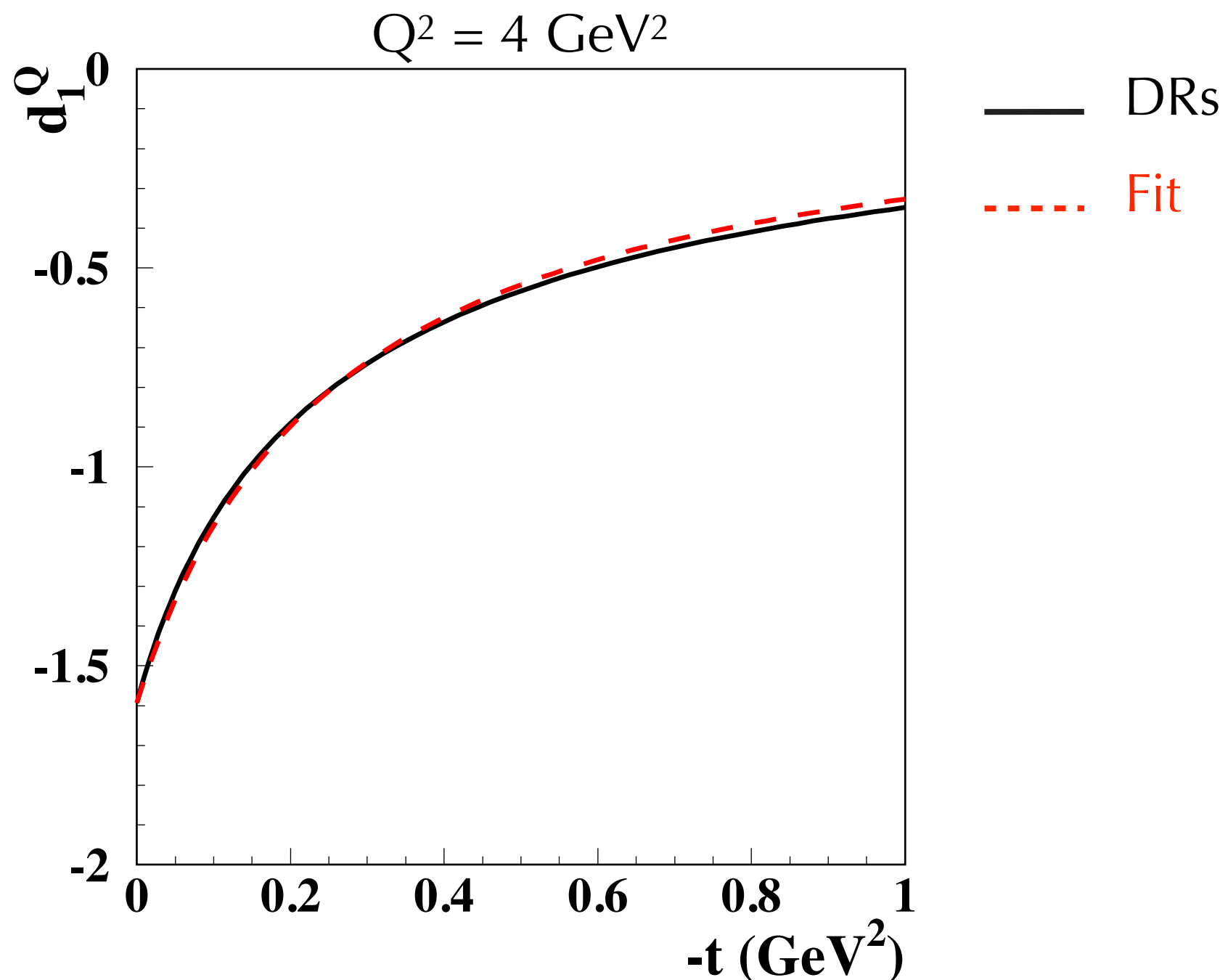
$$\text{subtracted DRs: } d_1^Q(t) = d_1^Q(0) - \frac{t}{\pi} \int_{4m_\pi^2}^{+\infty} dt' \frac{\text{Im}_t A_2(0, t', Q^2)}{t'(t'-t)}$$



subtraction constant to be fitted to data

D-term Form Factor: t-dependence

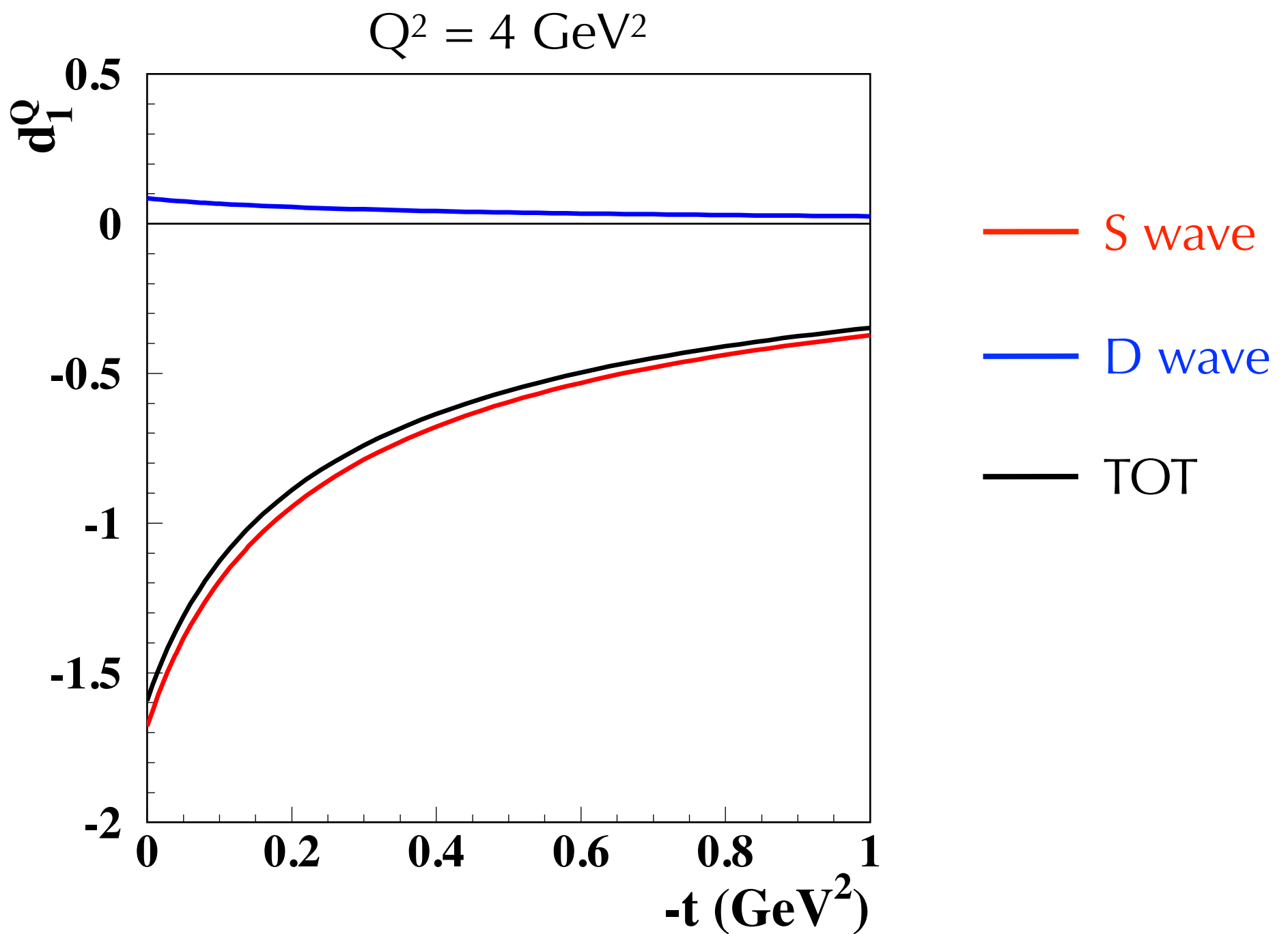
$Q = u + d$



Fit: $F^Q(t) = \frac{d_1^Q(0)}{[1 - t/(\alpha M_D^2)]^\alpha}$ with $M_D = 0.487 \text{ GeV}$
 $\alpha = 0.841$

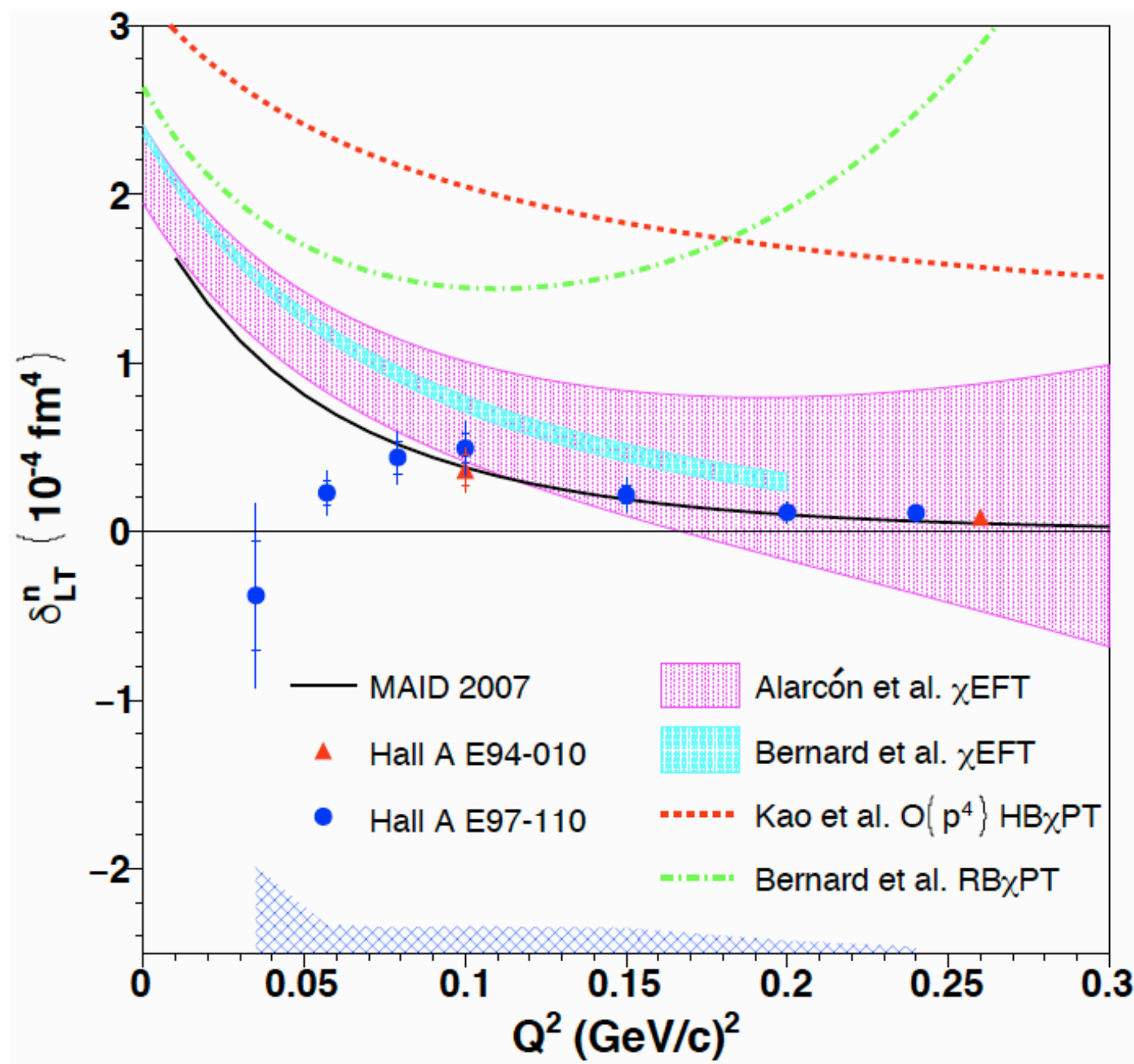
DR Results for D-term Form Factor

$Q = u + d$



VVCS Polarizabilities

$$\delta_{LT}(Q^2) = \frac{1}{2\pi^2} \int_{\nu_{thr}}^{\infty} \frac{K(\nu, Q^2)}{\nu} \frac{\sigma_{LT}(\nu, Q^2)}{Q\nu} d\nu$$
$$= \frac{e^2 4M^2}{\pi Q^6} \int_0^{x_0} x^2 [g_1(x, Q^2) + g_2(x, Q^2)] dx$$



VVCS Polarizabilities

$$\gamma_0(Q^2) = \frac{1}{2\pi^2} \int_{\nu_{thr}}^{\infty} \frac{K(\nu, Q^2)}{\nu} \frac{\sigma_{TT}(\nu, Q^2)}{\nu^3} d\nu$$

$$= \frac{e^2 4M^2}{\pi Q^6} \int_0^{x_0} x^2 [g_1(x, Q^2) - \frac{4M^2}{Q^2} x^2 g_2(x, Q^2)] dx$$

